國立臺灣大學生命科學院生態學與演化生物學研究所

碩士論文

Institute of Ecology and Evolutionary Biology

College of Life Science

National Taiwan University

Master Thesis

*Odysseus*基因對果蠅精子生成的影響

Characterization of *Odysseus* in *Drosophila* Spermatogenesis

吳家翔

Chia-Hsiang Wu

指導教授：丁照棣

Advisor: Chau-Ti Ting

中華民國102年1月

January, 2013

國立臺灣大學碩士學位論文
口試委員會審定書

*Odysseus*基因對果蠅精子生成的影響
Characterization of *Odysseus* in *Drosophila* Spermatogenesis

本論文係吳家翔君（學號R98B44009）在國立臺灣大學生態學與演化生物學研究所完成之碩士學位論文，於民國一百零二年一月廿二日承下列考試委員審查通過及口試及格，特此證明

口試委員：

台灣大學生態學與演化生物學研究所	丁照棣 博士	丁照棣
中央研究院生物多樣性研究中心	方　淑 博士	方淑
東海大學生命科學系	蔡玉真 博士	蔡玉真
長庚大學生物醫學系	皮海薇 博士	皮海薇

所長 [illegible]

中華民國102年1月22日

Acknowledgements

I would like to thank my advisor, Chau-Ti Ting, for all her guidance and immense patience. I am grateful for every opportunity she gave me to learn in her lab. Her infectious enthusiasm for science and truth always makes me wonder what it is like to be like that. I want to thank all the other members in Ting lab, especially Hsin-Yen Liu and Wen-Chiao Chan. They are always ready to help in every way and I do not think I could ever make it without them. My thanks also goes to the former members of Ting lab, Ya-Jen Cheng, Shi-Yow Yang, Chi-Chun Chen, Cheng-Lin Li, and Kevin Wei. I enjoyed and appreciated their company when I was too clumsy to know what to do.

I would like to thank Shu Fang and all the other members of Fang Lab at Academia Sinica. Without their help I would not be able to access facilities there (the Darkroom, especially). I also thank my committee members, Yu-Chen Tsai at Tunghai University and Haiwei Pi at Chang Gung University, for input and guidance to my thesis work. I thank the Core Facilities at ICOB, Academia Sinica, the DNA Sequencing Service at IBMS, Academia Sinica and the Technology Commons at National Taiwan University for technical support. I am grateful to Chuang-Yu Lin at ICOB for his help and advice about imaging, which is an important part of my work and I cannot thank him enough.

I thank Chung-I Wu for allowing me to visit his lab in spring and summer of 2011. I thank Mao-Lien Wu for her help at the bench and in daily life. My special thanks goes to Huyen Vu Thanh and her lovely family, Kimmy and Eric, for their hospitality and kindness. My roommates at 6128 S Dorchester Ave. were wonderful people and I owe them so much. My friends Yian and Artur should be awarded the Key to the City for humanitarian work in Chicago. They are heroes who save the Windy City.

I thank my college advisor, Shaw-Yhi Hwang, for all the cozy talks and nice coffee. I thank my friends for watching me and backing me up all the way: Jeff Lin, Tsung-Hsi Lin, Tzu-Wei Chan, Griffin Chang, Shi-Jun Chien, Wen-Che Tsai, Christy Lee, Eileen Lin, Flore Sun, Gennie Lin, and Tricia Lee. I am lucky and honored to meet long-time friends, Tien-Yin Huang, Cathy Hsu, and Wei-Che Hsu, in my early days when the friendship got started without self-interest. They are my most valuable assets.

Last but not least, I want to thank my family for their endless love and tolerance. Difficult kids who want to be a rebel at age 30 can be reeeeeally troublesome. For this I owe my life to them.

摘要

在物種形成的過程中，雜交不合（包括雜交不活與雜交不孕）能夠形成生殖屏障。因此，了解造成雜交不合的基因，將有助於認識物種的起源。*OdsH* 是由 *unc-4* 基因複製而產生的一個基因。在秀麗隱桿線蟲中，*unc-4* 與神經發育有關。*OdsH* 是造成兩近緣種果蠅——擬黃果蠅與模里西斯果蠅——雜交子代雄性不孕的主要因子，據信可能是因 $OdsH^{mau}$ 在精巢中異常表現、或因 $OdsH^{mau}$ 對擬黃果蠅的 Y 染色體異常結合所導致。在黃果蠅中，剔除 *OdsH* 使雄蟲生殖力下降；免疫染色實驗顯示，缺少 *OdsH* 表現的精巢，其生殖細胞數目較少。在本研究中，我測試了六株 *OdsH* RNAi 果蠅，其中四株來自果蠅品系中心，兩株為自行建立。我並使用了在特定位置表現綠色螢光蛋白的果蠅，標記精巢內部不同細胞，觀察 *OdsH* 對黃果蠅精子生成的影響。本研究展示六株 *OdsH* RNAi 果蠅的效果，有助於未來研究 *OdsH* 與 *unc-4* 的功能重疊。對黃果蠅精巢的觀察結果，則暗示 *OdsH* 可能參與精子生成當中的減數分裂與後期分化。

關鍵字：果蠅、基因重複、雜交不合、*OdsH* 基因、RNA 干擾、精子生成、*unc-4* 基因

Abstract

Hybrid incompatibility, including hybrid inviability and hybrid sterility, can act as a reproductive barrier in the process of speciation. Therefore, genes involved in hybrid incompatibility may provide a window on how new biological species form. The gene *Odysseus-site homeobox* (*OdsH*) is duplicated from *unc-4*, a homolog of a neuron developmental gene in *Caenorhabditis elegans*. *OdsH* has been identified as a crucial element that triggers hybrid male sterility in reciprocal crosses between two sibling species, *Drosophila simulans* and *D. mauritiana*. Previous studies have suggested that misexpression of $OdsH^{mau}$ in testes, or additional binding of $OdsH^{mau}$ to the Y chromosome of *D. simulans*, results in the hybrid sterility. In *D. melanogaster*, targeted gene knockout revealed that lack of *OdsH* expression reduces male fertility. Immunostaining in *OdsH* null mutant ($OdsH^{0}$) testes has shown a decrease in the number of germ cells. In this thesis, I generated two *OdsH* RNAi constructs and examined their efficiency with the other four available at stock centers. In addition, I used reporter lines that express enhanced green fluorescent protein to further characterize this testis-specific gene at the cellular level. My results demonstrated the efficiency of these RNAi strains, which should facilitate future studies on the functional redundancy between *OdsH* and *unc-4*. Cytological observation implies that *OdsH* may play a role in meiosis and terminal differentiation during spermatogenesis.

Keywords: *Drosophila*, gene duplication, hybrid sterility, *OdsH*, RNA interference, spermatogenesis, *unc-4*

Contents

List of Figures

List of Tables

Introduction

People have long been fascinated by the origin of species. From Aristotle (384 BC-322 BC) to Carl Linnaeus (1707-1778), philosophers strived to classify the creatures on Earth and assigned the order in which all lives are created. Conceivably, one of the earliest definitions of species pertains to the morphological similarity among individuals, because there is no more instinctive way to categorize lives than the observable and measureable traits by the naked eye. In face of vast numbers of species, people held different view on their origin. In the view of creationism, species today are just the same as they were when the Earth was formed. In contrast, some people doubted and questioned the possibility of creating new species. In the pre-Darwinian era, challenges against the deep-rooted ecclesiastical perspective begun emerging already. Such as Linnaeus, based on his classification work, pointed that a new species could arise from hybridizing plants. Jean-Baptiste Lamarck (1744-1829) also advanced the idea of hybridization as a source of new species (Reviewed in MCCARTHY 2008). By the time Charles Darwin (1809-1882) was born, the Age of Enlightenment came to an end. It was a society where reason was upheaved to the level comparable to church traditions, a society where research fellows received supports from state-funded academies, and a society where salons, coffee houses and debate clubs permeated.

Several keys contributed to Darwin's achievement in the theory of evolution: his immense curiosity and interest in natural history, the upper-class background and financially secure life that enabled him to be a gentleman scientist on HMS Beagle (1831-1836) (BROWNE 2009), and befriending his contemporary scientists, like Asa Gray (1810-1888), John Gould (1804-1881), John Herschel (1792-1871), Joseph Dalton Hooker (1817-1911) and Charles Lyell (1797-1875). Among them, Lyell's

uniformitarian view of geology—the same laws and processes of nature have always operated in the past and at present on Earth in the same way— helped shape Darwin's speculations on the "mystery of mysteries"(DARWIN 1859). Finally, a manuscript on natural selection from Alfred Russel Wallace (1823-1913) in 1858 gave impetus to the publication of Darwin's painstaking work and the cornerstone of evolutionary biology as well in 1859. In *On the Origin of Species*, Darwin proposed natural selection as the fundamental mechanism of evolution. It occurs when descents, from a common ancestor, carry heritable traits with variation related to fitness. Individuals with certain traits may have better chance to survive and reproduce than the others without. This can consequently lead to a specialized population, or a new species, that adapts to a particular way of life (DARWIN 1859).

Upon the arrival of Darwin's theory, the community was not ready for this radical idea. One reason that it came under suspicion was the absence of evidence to support. Although Gregor Mendel (1822-1884) published his seminal work on modern genetics in 1865, Darwin was not aware of it and failed to explicate his crossing experiment results with the blending inheritance and his pangenesis theory (Reviewed in CHARLESWORTH and CHARLESWORTH 2009). It was not until the turn of the 20th century that Mendel's laws were rediscovered and advocated by Hugo de Vries (1848-1935), Carl Correns (1864-1933), Erich von Tschermak (1871-1962) and William Bateson (1861-1926) (Reviewed in KEYNES and COX 2008). Yet the evolution and species problems were not all solved happily ever after. For example, Bateson, an English biologist who coined the term "genetics," did not lend support to Darwin's idea. In fact, since the renaissance of Mendelian inheritance, there were dissenting voices from Darwin's natural selection. These voices, including de Vries and Bateson, believed that

a new species arises from mutations that cause large, discontinuous modification of individuals. This theory—referred to as mutationism or Mendelism—was defied by the biometricians, who followed Darwin's view and concentrated on small, continuous variations among individuals (Reviewed in AYALA and FITCH 1997). About the same time, explosive progress in genetics enabled scientists to trace the inheritance factors in cells. Thomas Hunt Morgan (1866-1945) used *Drosophila melanogaster* to demonstrate the chromosome theory of inheritance proposed by Walter Sutton (1877-1916) and Theodor Boveri (1862-1915). For the first time, a gene was showed physically on a specific chromosome as a carrier of traits. The Morgan group—including his students Alfred Sturtevant (1891-1970), Calvin Bridges (1889-1938) and Hermann Joseph Muller (1890-1967)—became the trailblazer for the further understanding of modern genetics. Together, they established what is common knowledge for geneticists today, such as genetic linkage, polytene chromosome map and X-ray mutagenesis (Reviewed in DAVIS 2004).

The mutationist-biometrician contradiction was reconciled by the introduction of mathematical statistics into genetics in the 1920s and 1930s. Ronald Fisher (1890-1962), Sewall Wright (1889-1988), and John Burdon Sanderson Haldane (1892-1964) were among the most influential figures that developed the theoretical framework of population genetics. Their work demonstrated that natural selection could act on small, continuous variations that are passed on from parents to offspring through Mendelian inheritance and contribute to morphological and functional alterations. Furthermore, it led to the demise of mutationism and stimulated the forthcoming synthetic theory of evolution, the Modern Synthesis (Reviewed in AYALA and FITCH 1997; CHARLESWORTH and CHARLESWORTH 2009).

At the dawn of the Modern Synthesis era, two prominent scientists, Theodosius Dobzhansky (1900-1975) and Ernst Mayr (1904-2005), made tremendous contribution in combining the evolution theory and multiple scientific disciplines. Both of them proposed what is known as the biological species concept: species are natural populations that are able to interbreed and reproductively isolated from other such populations. Since then, the discussion about isolating mechanisms has been the core to decode speciation (DOBZHANSKY 1937; MAYR 1942). In 1936, Dobzhansky published his groundbreaking work in the genetics of speciation (DOBZHANSKY 1936). He crossed two species, *D. pseudoobscura* and *D. persimilis*, and backcrossed the fertile F_1 females to males of the two species. He thus obtained hybrids with many combinations of heterospecific chromosomes. With the help of visible markers, the fertility of these hybrids, which was measured by the testis size, indicated which region on whose chromosome caused hybrid sterility—a reproductive barrier that is required to create a new species. Dobzhansky gave empirical evidence that genes, instead of cytoplasm difference or chromosome rearrangement, cause hybrid sterility. Also, through this experiment, he provided an answer to Darwin's paradox: how can sterility or inviability survive through natural selection? Dobzhansky proposed an interaction between (at least) two loci responsible for hybrid sterility: Assume two allopatric populations with the same genotype *aabb*. Then a mutation occurs: now one population comprises *Aabb* and *AAbb*, while the other comprises *aaBb* and *aaBB*. The new allele *A* is compatible with *b*, and *B* is compatible with *a*. In this scenario, allele *A* and *B* are never put to the test together. When the two populations meet, the incompatibility between *A* and *B* can lead the hybrid offspring to a dead end. This idea, also discussed and contributed by William Bateson (1909) and H. J. Muller (1942), has become known as the

Bateson-Dobzhansky-Muller Model (Reviewed in ORR 1996).

Dobzhansky's pioneering experiment did not add zest to the seeking of hybrid incompatibility genes. Conversely, interest in this subject was not revived until early 1980s, when Jerry Coyne launched the study to answer the genetic basis of hybrid male sterility between *D. simulans* and *D. mauritiana* (COYNE 1984; JOHNSON 2008). Coyne and Charlesworth (1986) further traced the largest sterility effect to the X chromosome and found it closely linked to the marker, *forked*. Using molecular markers, Perez et al. (1993) were able to associate the sterility effect to a major locus and named it *Odysseus* (*Ods*). The name "Odysseus"—the hero who devised the wooden horse that destroyed the city of Troy in the Homeric epic—is metaphorical: the *D. mauritiana* allele invades the *D. simulans* background and finally leads to a crash of the lineage. A subsequent investigation of *Ods* revealed that Ods^{mau} alone cannot cause sterility; only when Ods^{mau} and its distal region were cointrogressed, the sterility effect can be fully exerted (PEREZ and WU 1995). Finally, an attempt of fine-scale genetic mapping successfully delineated the *Ods* locus to the nucleotide level (TING *et al.* 1998). The location of *Ods* was defined by two introgression lines from a collection of 190 newly generated recombinants: 99F (the fertile line that has the longest introgressed fragment from *D. mauritiana*) and 193S (the sterile line that has the shortest introgressed fragment from *D. mauritiana*), which differ only by a 3-kb region where reside the (later known) exons 3 and 4 of a gene. Since this gene contains a homeobox in the exons 2 and 3, it was named *Odysseus-site homeobox* gene (*OdsH*).

The discovery of *OdsH* has posed several questions: First, sequence analysis showed that *OdsH*, particularly its homeodomain, has undergone rapid evolution, which is asymmetric to its highly conserved paralog, *unc-4* (TING *et al.* 1998). Second, the fact

that the male reproductive organ-specific *OdsH* duplicated from the neuron-specific *unc-4* (TABUCHI *et al.* 1998) supports a hypothesis that a duplicated gene, which is liable to functional divergence and has not reached its stable maintenance, is a candidate "speciation gene" (TING *et al.* 2004). Third, since the maladaptive defect induced by *OdsH* in hybrids is an evolutionary by-product, what is the normal function of *OdsH*? In *D. melanogaster*, *OdsH* is suggested to enhance sperm production, probably by speeding up sperm maturation (SUN *et al.* 2004) and/or maintaining germline stem cells (CHENG *et al.* 2012). Fourth, what is the mechanism underlying the hybrid sterility? The homeodomain motif supports an educated guess that *OdsH* is a DNA-binding transcription factor. The misregulated *OdsH* in *D. simulans-D. mauritiana* hybrid sterile line disrupts the expression of genes involved in spermatogenesis, which may be the cause of spermatogenic failure (LU *et al.* 2010; SUN *et al.* 2004). However, Bayes and Malik reported an additional heterochromatic localization of $OdsH^{mau}$ on the Y chromosome of *D. simulans* may cause chromosome decondensation in sterile hybrids, which suggests a "gain-of-function" protein-DNA interaction that echoes the Bateson-Dobzhansky-Muller Model (BAYES and MALIK 2009).

In this thesis, I tested four *OdsH* RNAi strains available from stock centers and two that newly generated at my hands. I used reporter lines that express green fluorescent protein (GFP) to characterize this testis-specific gene at the cellular level. These efforts are intended to tackle two questions: (1) The function redundancy between *OdsH* and its paralog, *unc-4*, and (2) The specific role of *OdsH* in *D. melanogaster* spermatogenesis. Together, this thesis provides some new hints on genes involved in hybrid incompatibility and materials for future study.

Materials and Methods

Fly strains and husbandry

All *Drosophila* strains were raised at 25˚C on standard cornmeal medium. *his*-GFP (CLARKSON and SAINT 1999), *sa*-GFP (CHEN *et al.* 2005) (a gift from Margaret T. Fuller at Stanford University), and *bamP*-GFP (CHEN and MCKEARIN 2003) (a gift from Haiwei Pi at Chang Gung University) were crossed to $OdsH^{+}$ and $OdsH^{0}$ flies (SUN *et al.* 2004) to visualize germ cells in different developmental stages of spermatogenesis. *UAS-*$OdsH^{RNAi}$ strains were obtained from the Vienna *Drosophila* RNAi Center at the Campus Vienna Biocenter (GD51289 and KK103949) and the Transgenic RNAi Project at the Harvard Medical School (JF02198 and HMS01554). GMR>$OdsH^{mel}$ was used for testing RNAi efficiency. *D. melanogaster* y^{1} sc^{1} v^{1} *P{nos-phiC31\int.NLS} X; P{CaryP}attP2* was provided by Rainbow Transgenic Flies, Inc. (Camarillo, CA) and used for transgenesis. *FM6* was used to make homozygous *sa*-GFP, $OdsH^{+}$ and *sa*-GFP, $OdsH^{0}$ flies. See Table 1 for strain information.

Synthesis of mir-6-1-based microRNA for RNAi constructs

The design of mir-6-1-based miRNA against *OdsH* was based on Chen et al. (2007). A target site on $OdsH^{sim}$ coding region was selected according the criteria as follows: (1) a 22-nucleotide sequence, (2) a 30-52% guanine-cytosine content, (3) at least three adenine-thymine within the 16^{th} to 20^{th} nucleotide, (4) an adenine at the 20^{th} nucleotide, (5) no guanine at the 13^{th} nucleotide, (6) an adenine at the 3^{rd} nucleotide (optional), and (7) an thymine at the 10^{th} nucleotide (optional). The resulting 22-nt sequence was then swapped to the Oligos 1 and 2 cassettes with the 20^{th} nucleotide in the Oligo 1 replaced by cytosine. Then, the last four nucleobases of the Oligo 2 were

changed to the reverse-complement counterpart of the last four nucleobases of the modified 22-nt sequence in Oligo 1. Anneal Oligos 1 and 2 by the first-round PCR using Expand High Fidelity^{PLUS} PCR System (Roche), which generated the mir-6-1 mimic sequence that later formed the miRNA precursors (Figure 1, A). This product was amplified by the second-round PCR with Oligos 3 and 4, which added the mir-6-1 flanking sequences and restriction recognition sites *Not*I/*Bgl*II and *Bam*HI/*Xba*I at 5-prime and 3-prime ends respectively (Figure 1, B and C). The resulting PCR-amplified fragment was confirmed by sequencing after cloned into pCR™4-TOPO® TA vector (Invitrogen) and the construct was named mir-6-1-OdsH^{simA}. By the same method the constructs mir-6-1-OdsH^{simB}, mir-6-1-OdsH^{mauA} and mir-6-1-OdsH^{mauB} were generated. See Table 2 for oligo sequences.

Table 1. Fly strains used in this thesis.

Strain	Genotype	Note
w^{1118}	w^{1118}	
FM6	*FM6,* y^1 dm^+ w^1*/Dp(1;Y)*y^+	Bloomington stock 4327
$OdsH^+$	w^{1118} $OdsH^+$	SUN *et al.* (2004)
$OdsH^0$	w^{1118} $OdsH^0$	SUN *et al.* (2004)
GMR>$OdsH^{mel}$	w^**; P{GAL4-ninaE.GMR}12; P{*w^+ *UAS-*$OdsH^{mel}$ *9B}*	LIN (2009)
his-GFP	w^{1118}*; P{His2Av*$^{T:Avic\GFP-S65T}$*}62A*	CLARKSON and SAINT (1999); Bloomington stock 5941
sa-GFP	*y w P{*w^+ *sa-GFP}*	CHEN *et al.* (2005)
bamP-GFP	*hsFLP; Sp/Cyo; P{*w^+ *-898/+133-bam:GFP}*	CHEN and MCKEARIN (2003)
GD51289	w^{1118}*; P{*w^+ *GD51289}*	*UAS-*$OdsH^{RNAi}$ from VDRC
KK103949	w^{1118}*; P{*w^+ *KK103949}*	*UAS-*$OdsH^{RNAi}$ from VDRC
JF02198	y^1 v^1*; P{TRiP.JF02198}attP2*	*UAS-*$OdsH^{RNAi}$ from TRiP
HMS01554	y^1 sc^* v^1*; P{TRiP.HMS01554}attP2*	*UAS-*$OdsH^{RNAi}$ from TRiP
attP2	y^1 sc^1 v^1 *P{nos-phiC31\int.NLS}X; P{CaryP}attP2*	NI *et al.* (2008); Bloomington stock 25710

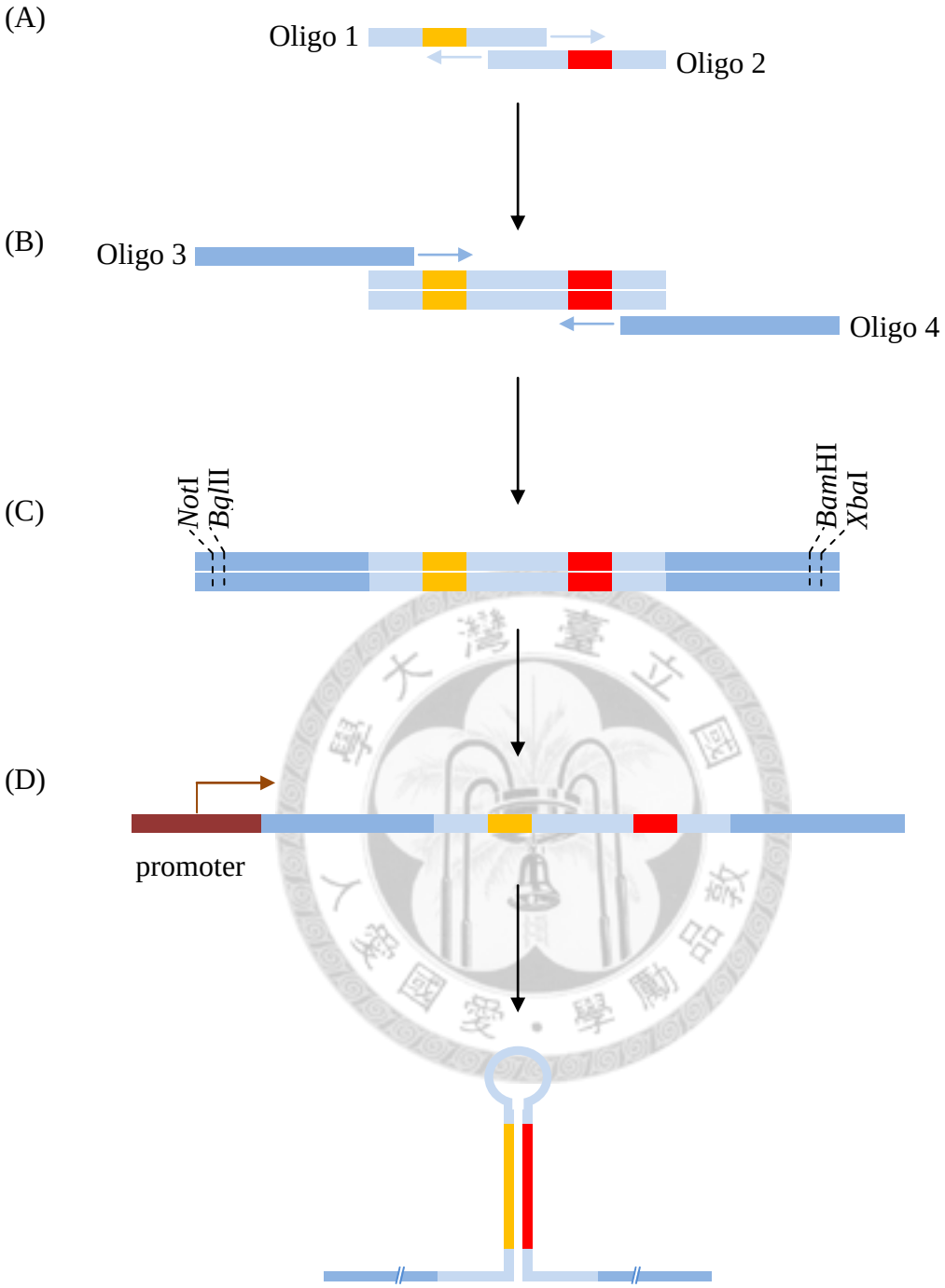

Figure 1. Synthesis of mir-6-1-based microRNA. (A) Oligos 1 and 2, embedded a 22-nt sequence (yellow and red) that targets against the gene of interest, are annealed by the first-round PCR. (B) Oligos 3 and 4 are used to amplify the first-round PCR product, creating (C) a ~230-bp fragment flanked by *Not*I/*Bgl*II and *Bam*HI/*Xba*I sites at 5-prime and 3-prime end, respectively. (D) As the miRNA template placed under the control of a promoter is transcribed, the hairpin-structured primary miRNA forms. This artificial primary miRNA then enters the endogenous RNAi pathway and acts as a functional miRNA.

Table 2. Oligo names and sequences used in this thesis.

Name	Sequence (5′ to 3′)
"Oligo 1" for mir-6-1-based RNAi synthesis	
miR6_OdsHsim_A1	GGCAGCTTACTTAAACTTAATCACAGCCTTTAATGTATAGCGGTTTGGTGTCAAACTATAAGTTAATATACCATATC
miR6_OdsHsim_B1	GGCAGCTTACTTAAACTTAATCACAGCCTTTAATGTAAATCGTCCTTCAGCATCACATTAAGTTAATATACCATATC
miR6_OdsHmau_A1	GGCAGCTTACTTAAACTTAATCACAGCCTTTAATGTGGAGAAAGCCTTCCAGGAACATTAAGTTAATATACCATATC
miR6_OdsHmau_B1	GGCAGCTTACTTAAACTTAATCACAGCCTTTAATGTTCGAGGATATGGAAGTGGACGTTAAGTTAATATACCATATC
"Oligo 2" for mir-6-1-based RNAi synthesis	
miR6_OdsHsim_A2	AATAATGATGTTAGGCACTTTAGGTACATAGCGGTTTGGTGTCAAAATATAGATATGGTATATTAACTTATAGT
miR6_OdsHsim_B2	AATAATGATGTTAGGCACTTTAGGTACAAATCGTCCTTCAGCATCAAATTAGATATGGTATATTAACTTAATGT
miR6_OdsHmau_A2	AATAATGATGTTAGGCACTTTAGGTACGGAGAAAGCCTTCCAGGAAAATTAGATATGGTATATTAACTTAATGT
miR6_OdsHmau_B2	AATAATGATGTTAGGCACTTTAGGTACTCGAGGATATGGAAGTGGAAGTTAGATATGGTATATTAACTTAACGT
"Oligo 3" and "Oligo 4" for mir-6-1-based RNAi synthesis	
mi6_5′ NotI_BglII	GGCGCGGCCGCCGCCAGATCTTTTAAAGTCCACAACTCATCAAGGAAAATGAAAGTCAAAGTTGGCAGCTTACTTAAACTTA
mi6_3′ BamHI_XbaI	GGCCTCTAGAACGGATCCAAAACGGCATGGTTATTCGTGTGCCAAAAAAAAAAAAAAATTAAATAATGATGTTAGGCAC
"LA_F" and "LA_R" for recombineering	
VALIUM_GYPSY_L_F	AGGCGCGCCTCGGTACACTAGTTG
VALIUM_GYPSY_L_R	CGCGGATCCTACTAGTGTTGTTGG
"RA_F" and "RA_R" for recombineering	
VALIUM_GYPSY_R_F	CGCGGATCCGCGTGCAGTGGCCAC
VALIUM_GYPSY_R_R	ACCTTAATTAAGAGCTCCTGCAGGTTG
"5'-Check-F" and "5'-Check-R" for recombineering	
pacman_L for VGL	GTGAGCGCGCGTAATACGACTCAC
VALIUM20_22_R	TAATCGTGTGTGATGCCTACC
for OdsH^{mel} expression check by RT-PCR	
OdsH c0+	GCAAAAGCTAAGACGAAAATGGAT
U8 4524-	TGCTTAGCTAACCACCCGAAATCA
rp49F	CAGTCGGATCGATATGCTAAGCTGT
rp49R	TTACCGACCTTGGGCATCAGATACT

Generation of RNAi strains against *OdsH*^{sim} and *OdsH*^{mau} in *D. melanogaster*

Two mir-6-1-based constructs, together with the vector Valium22 (NI *et al.* 2011) (Figure 2), were combined by a three-way ligation with appropriate restriction enzyme digestions, which created pV22_OdsH^{simAB} (Figure 3). pV22_OdsH^{mauAB} was generated by the same method (Figure 4). These two resulting constructs were then microinjected into embryos of *attP* flies (Bloomington Stock 25710) via ΦC31 integrase-mediated transformation by Rainbow Transgenic Flies, Inc. Hatched virgin adults (P_0) were sexed and mated with the parental *attP* virgin flies, and transformants were screened in F_1 flies to create homozygous stocks.

Immunostaining

Immunostaining was performed as described (SINGH and HOU 2008) with minor modifications. Testes were dissected in *Drosophila* ringer's solution and fixed in 4% paraformaldehyde made in phosphate-buffered saline (PBS) for 20 minutes. Fixed samples were washed three times for 20 minutes each with 1 × PBST (0.1% Triton X-100 in 1 × PBS), and blocked in 1 min blocking buffer (Bio-Cando) at 4°C overnight. Samples were then incubated in primary antibody at 4°C overnight, washed five times for 30 minutes each with 1 × PBST, and incubated in secondary antibody at room temperature for two hours in the dark. After 5 washes in 1 × PBST and another three washes in 1 × PBS, samples were mounted on slides with a drop of mounting medium (50% glycerol in 1 × PBS) and stored at 4°C until imaging.

Primary and secondary antibodies were diluted in the blocking buffer. Primary antibodies used were: 1:50 mouse anti-Fasciclin III (Developmental Studies Hybridoma Bank, DSHB), and 1:10,000 rabbit anti-GFP (Torrey Pines Biolabs). Alexa fluorescence

conjugated secondary IgG (H+L) antibodies were used at 1:200 for goat anti-rabbit 488 and 568 (Molecular Probes).

Imaging and quantification

Fluorescence images of testes were obtained using the Leica TCS SP5 AOBS confocal microscope. Signals were analyzed using MetaMorph (Molecular Devices) software. Image stacks were converted into 3D objects by 4D viewer, and signal intensity was estimated by summing the number of voxels within the regions of interest. Light microscope images of compound eyes were obtained using Zeiss SteREO Lumar.V12. Compound eye size was measured using MetaMorph software. Scanning electron microscope images of compound eyes were obtained using the FEI Inspect S in low vacuum mode.

Statistical methods

Statistical significance of the differences in average volume of green fluorescent signals per testis and in average compound eye size and circumference of various genotypes was estimated using the Mann-Whitney *U* test.

RNA extraction and cDNA reverse transcription

Total RNA was extracted from five three-day-old adult male flies with TRIzol reagent (Invitrogen) following the manufacturer's instructions. cDNA was synthesized using SuperScript® III First-Strand Synthesis System for RT-PCR (Invitrogen) according to the manufacturer's protocol with $OdsH^{mel}$-specific primers. *Drosophila ribosomal protein 49* gene (*rp49*) was used as a loading control. PCR conditions

included one cycle of 2 min at 95℃ followed by 25 cycles of 95℃ for 30 s, 55℃ for 90 s and 72℃ for 30 s, and a final incubation at 72℃ for 10 min. PCR products were separated on 0.8% agarose gels. See Table 2 for primer sequences.

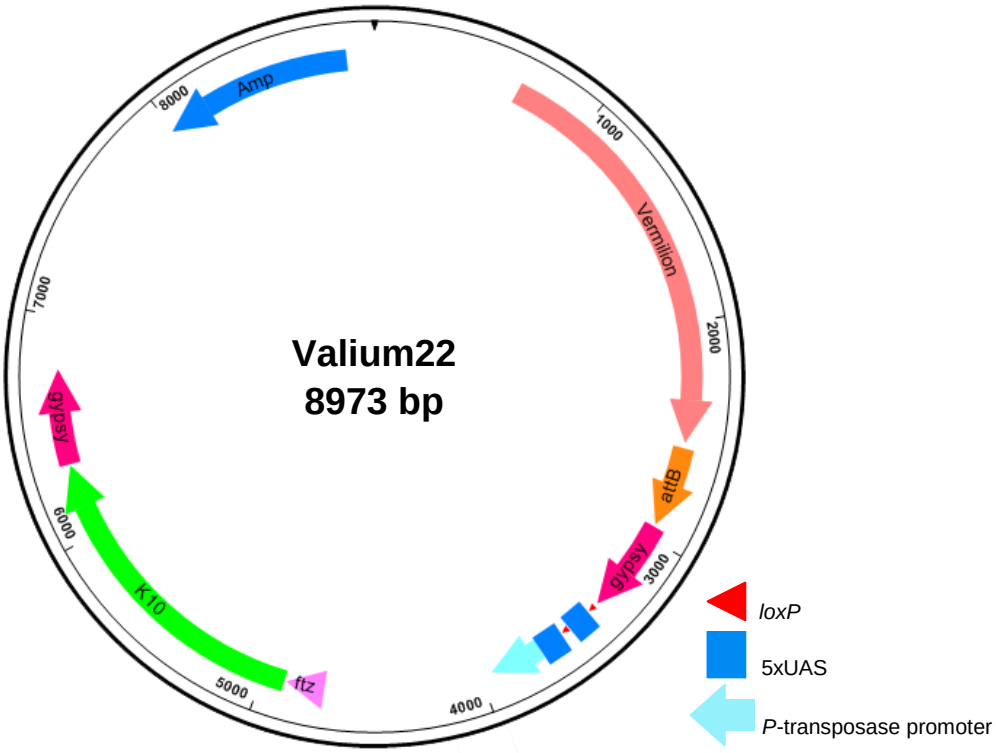

Figure 2. Valium22 vector. Valium22 is a ΦC31-based transformation vector and specialized for expression in the female germline. ftz, the 3-prime UTR intron of *fushi tarazu*, contains the transport and localization signal. K10, the 3-prime UTR of *female sterile (1) K10*, contains the localization element. The whole design is flanked by two gypsy insulators to stabilize transgenic expression.

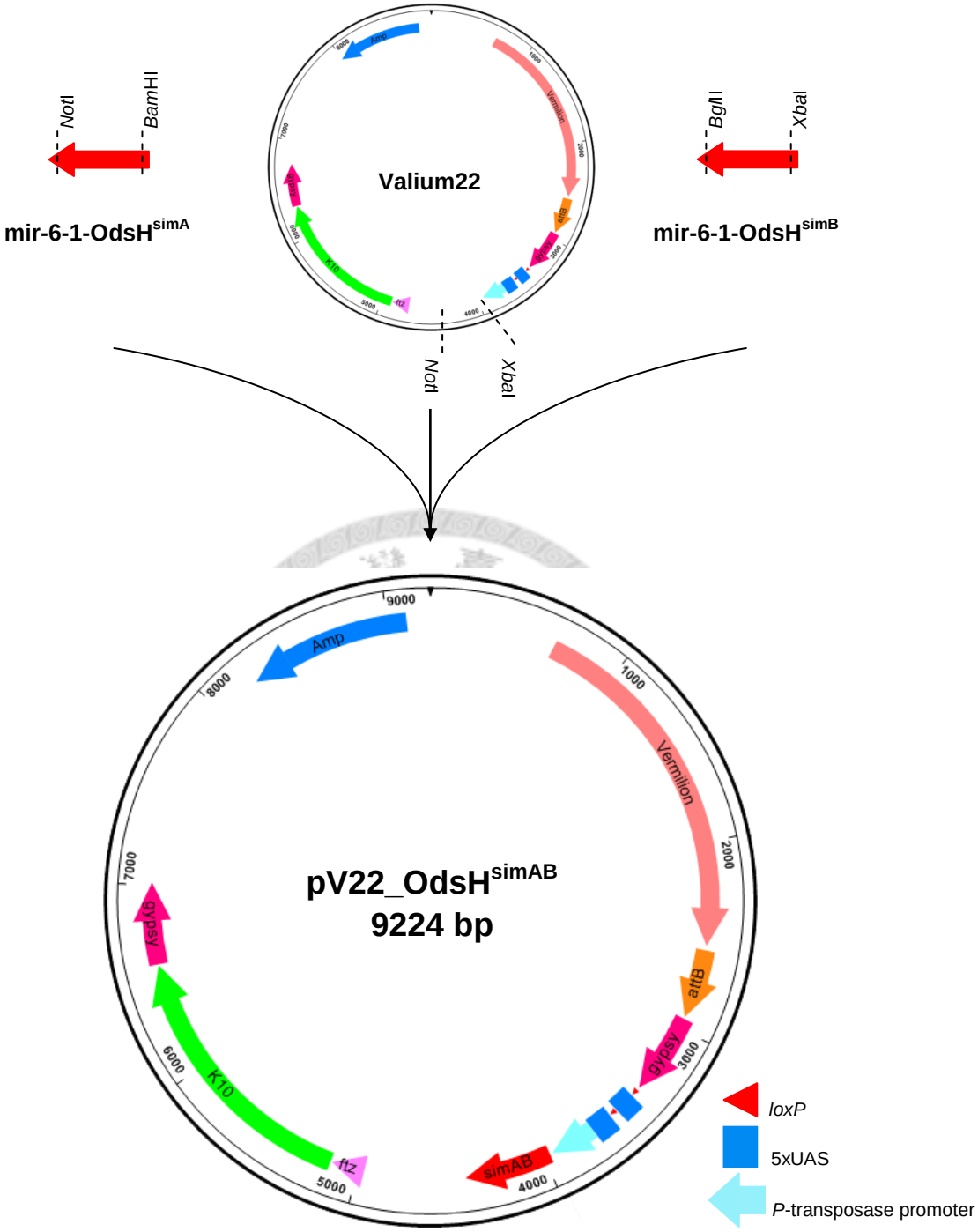

Figure 3. Generation of pV22_OdsH^{simAB}. Two synthetic miRNA templates and the vector Valium22 were digested with different restriction enzyme pairs: *Xba*I/*Bgl*II, *Bam*HI/*Not*I, and *Xba*I/*Not*I. These three fragments were then combined in a three-way ligation to create pV22_OdsH^{simAB} for ΦC31 integrase-mediated transformation.

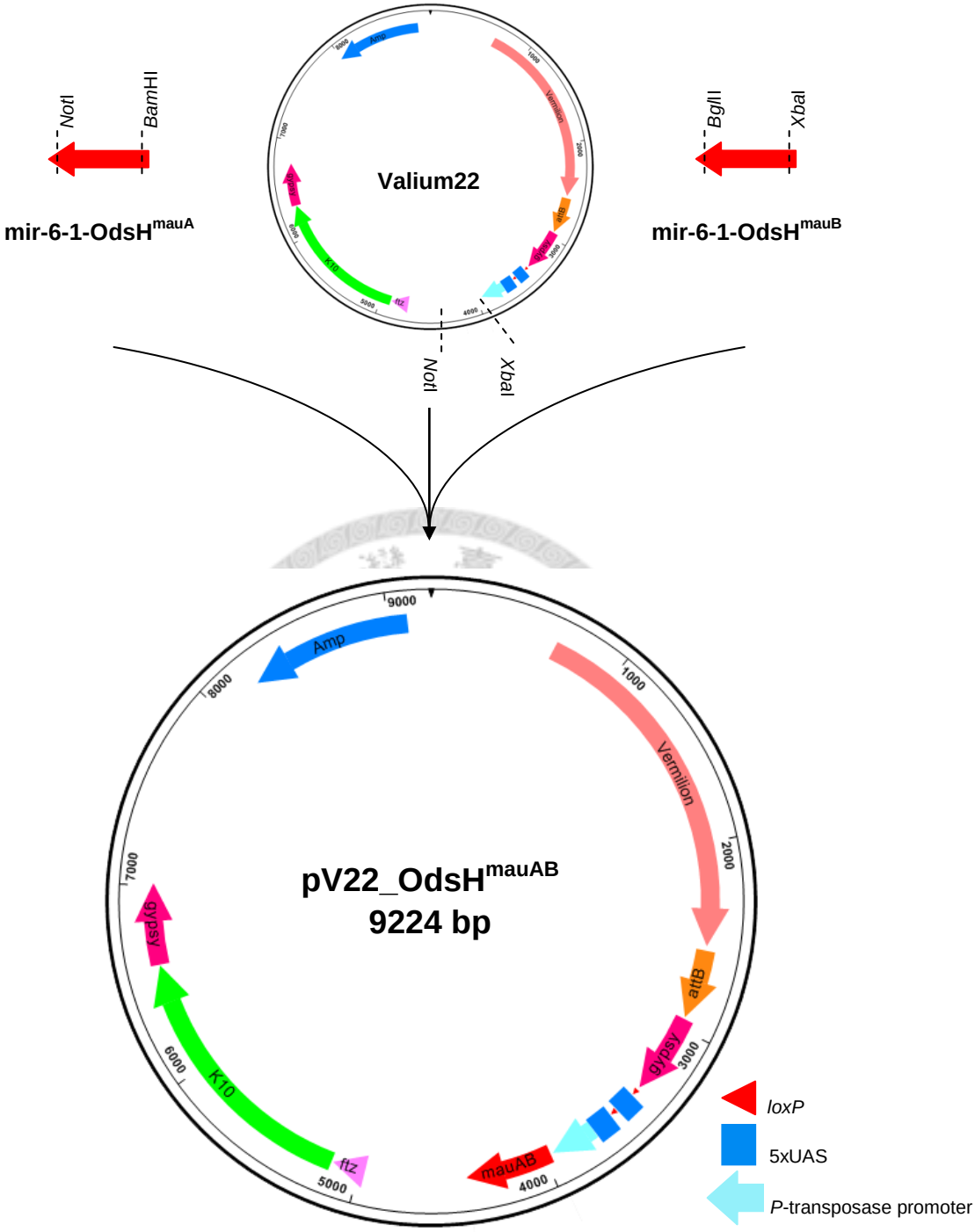

Figure 4. Generation of pV22_OdsH^{mauAB}. Two synthetic miRNA templates and the vector Valium22 were digested with different restriction enzyme pairs: *Xba*I/*Bgl*II, *Bam*HI/*Not*I, and *Xba*I/*Not*I. These three fragments were then combined in a three-way ligation to create pV22_OdsH^{mauAB} for ΦC31 integrase-mediated transformation.

Results

Generation of RNAi strains against *OdsH*^{sim} and *OdsH*^{mau} in *Drosophila melanogaster*

The mir-6-1-based RNAi constructs, pV22_OdsH^{simAB} and pV22_OdsH^{mauAB}, were introduced into *D. melanogaster* y^1 sc^1 v^1 *P{nos-phiC31\int.NLS}X; P{CaryP}attP2* embryos. For the pV22_OdsH^{simAB} construct, 63.1% of hatched larvae eclosed, 82.9% of the adults were fertile, and 26.5% of the fertile adults were transformants. For the pV22_OdsH^{mauAB} construct, 60% of hatched larvae eclosed, 70.8% of the adults were fertile, and 29.4% of the fertile adults were transformants (Table 3). Two *UAS-OdsH*^{RNAi} strains were therefore generated and named *OdsH*$^{RNAi\_simAB}$ and *OdsH*$^{RNAi\_mauAB}$.

RNAi knockdown rescues the *OdsH*^{mel} ectopic expression phenotype in *Drosophila* eye

A total of six *UAS-OdsH*^{RNAi} strains, including two newly generated and four obtained form stock centers, were investigated in the *GMR-Gal4>UAS-OdsH*^{mel} background. Observations on *Drosophila* eye phenotypic changes demonstrate that all the six RNAi strains yield the knockdown effect. Compared to the wild-type eyes (Figure 5, A-A′), GMR-driven *OdsH*^{mel} caused severe eye defects: reduction in size, and loss of ommatidia and bristles (Figure 5, B-B′). The two VDRC and two TRiP lines restored the eye defects evidently (Figure 5, C-F′). All of them displayed a wild-type-like eye of normal size. However, only three of them showed regular ommatidia and bristles (Figure 5, D-F′), except for the strain GD51289, which produced fused ommatidia and disorganized bristles (Figure 5, C-C′). The newly synthesized

OdsH$^{RNAi\_simAB}$ and *OdsH*$^{RNAi\_mauAB}$, whose guide and passenger strands are based on the coding sequences of *OdsH*^{sim} and *OdsH*^{mau}, showed minor but palpable knockdown effect. In the *GMR-Gal4>UAS-OdsH*^{mel} background, *OdsH*$^{RNAi\_simAB}$ and *OdsH*$^{RNAi\_mauAB}$ partially restored not only the size of compound eyes but also the growth of ommatidia and bristles (Figure 5, G-G′ and H-H′). Measurements of eye area and circumference provide quantification results in strong agreement with phenotypic observations that the four strains from stock centers had higher efficiency than the two self-made (Figures 6 and 7).

To further confirm the rescue effect, I used RT-PCR to detect the *OdsH*^{mel} mRNA level of the above-mentioned strains. The result showed that the VDRC and TRiP stocks obviously reduced *OdsH*^{mel} expression towards the wild-type (*w*^{1118} and GMR-Gal4) level. It is expected that the decrease of *OdsH*^{mel} mRNA was ambiguous in *OdsH*$^{RNAi\_simAB}$ and *OdsH*$^{RNAi\_mauAB}$, whose RNAi constructs were designed according to *OdsH*^{sim} and *OdsH*^{mau} coding sequences, because *OdsH* has experienced rapid evolution and diverged at the sequence level (Figure 8).

Table 3. Summary of the introduction of mir-6-1-based RNAi constructs into *Drosophila melanogaster* via ΦC31 integrase-mediated recombination. *Only a part of the hatched larvae were delivered by Rainbow Transgenic Flies, Inc.

Symbol	Genotype	Hatching rate (larvae/injected eggs)	Eclosing rate (P_0 adults/larvae)	Fertility rate (fertile P_0 adults/P_0 adults)	Transformation rate (transformants/fertile P_0 adults)
$OdsH^{RNAi\_simAB}$	$y^1\ sc^1\ v^1; P\{OdsH^{RNAi\_simAB}\}attP2$	*	63.1% (41/65)	82.9% (34/41)	26.5% (9/34)
$OdsH^{RNAi\_mauAB}$	$y^1\ sc^1\ v^1; P\{OdsH^{RNAi\_mauAB}\}attP2$	*	60% (24/40)	70.8% (17/24)	29.4% (5/17)

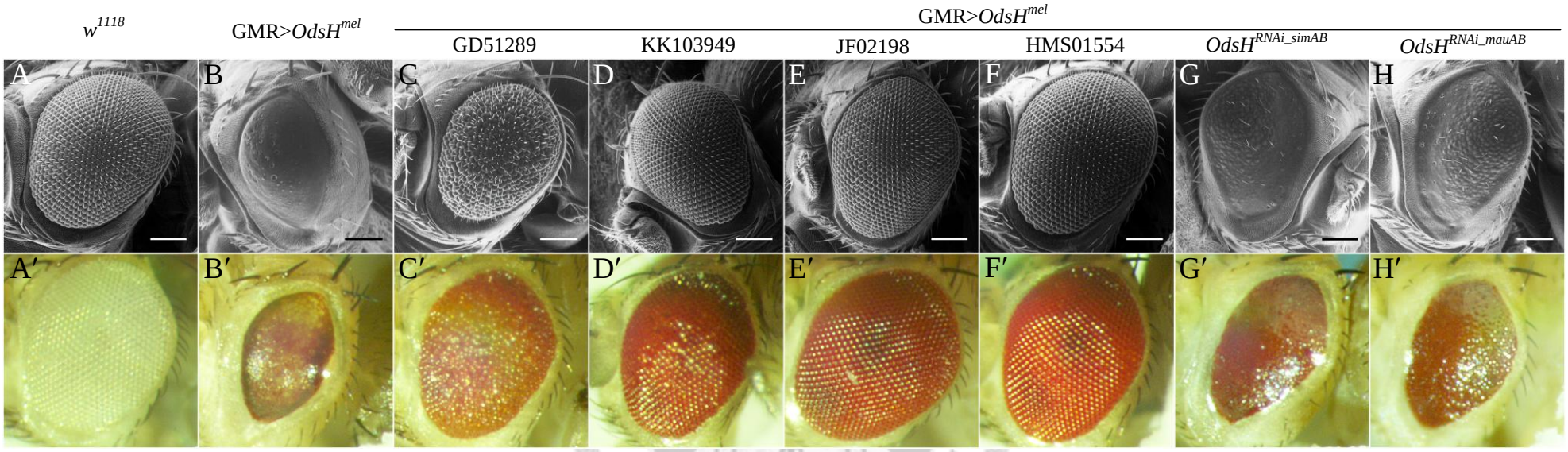

Figure 5. *Drosophila* eye images from wild-type and transgenic flies. (A-H) Scanning electron microscope images. (A′-H′) Light microscope images. (A-A′) w^{1118}. (B-B′) GMR>$OdsH^{mel}$. (C-C′) GMR>$OdsH^{mel}$; GD51289 (VDRC). (D-D′) GMR>$OdsH^{mel}$; KK103949 (VDRC). (E-E′) GMR>$OdsH^{mel}$; JF02198 (TRiP 1st Gen.). (F-F′) GMR>$OdsH^{mel}$; HMS01554 (TRiP 2nd Gen.). (G-G′) GMR>$OdsH^{mel}$; $OdsH^{RNAi\_simAB}$. (H-H′) GMR>$OdsH^{mel}$; $OdsH^{RNAi\_mauAB}$. Scale bars: 100 μm.

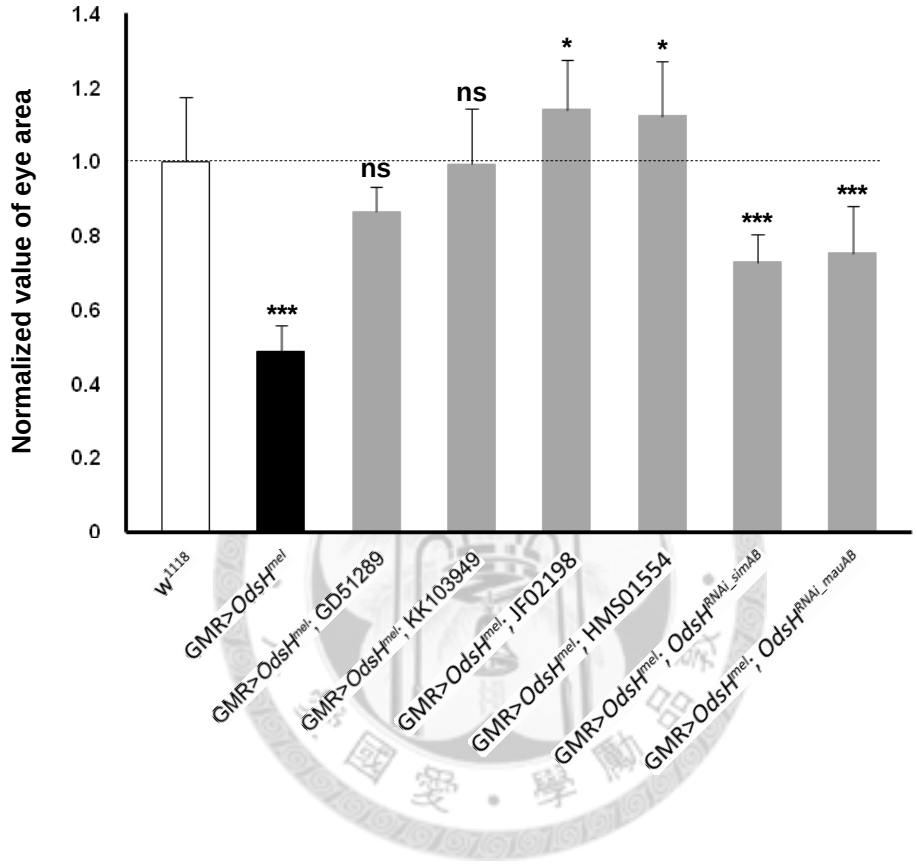

Figure 6. Normalized values of eye area to *w*^{1118} control. Genotypes are indicated below the graph. Error bars indicate the standard deviation of the mean. Statistical significance was determined with the Mann-Whitney *U* test. *, $P < 0.05$; ***, $P < 0.001$; ns, not significant. n = 10 testes for each data point.

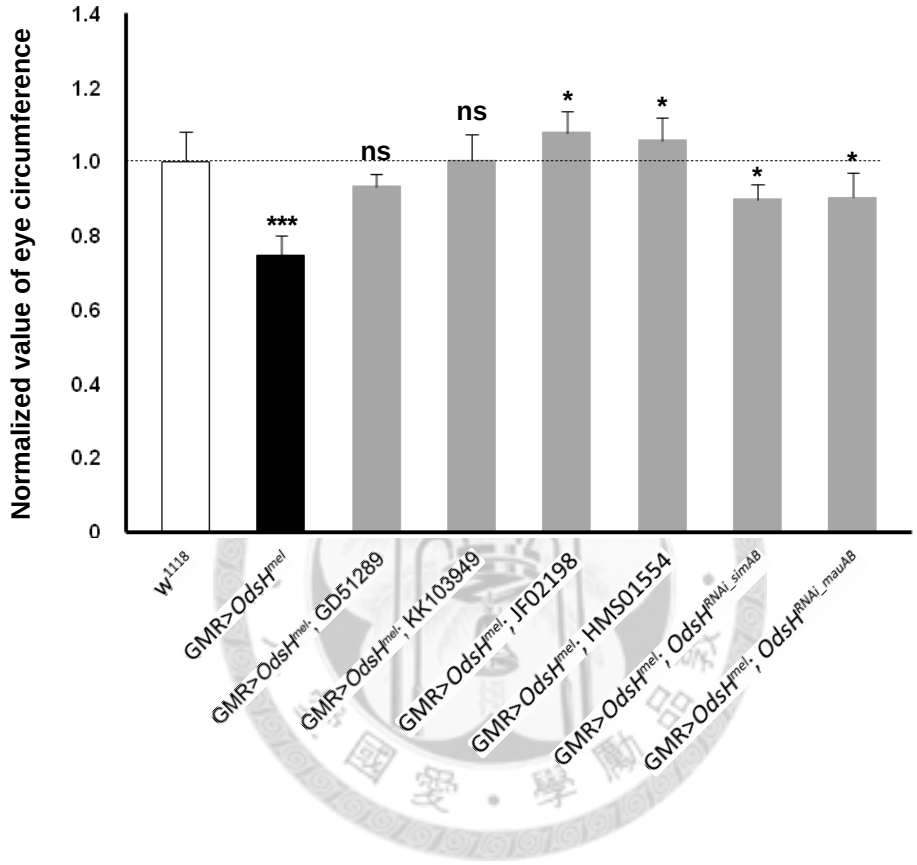

Figure 7. Normalized values of eye circumference to w^{1118} control. Genotypes are indicated below the graph. Error bars indicate the standard deviation of the mean. Statistical significance was determined with the Mann-Whitney *U* test. *, $P < 0.05$; ***, $P < 0.001$; ns, not significant. n = 10 testes for each data point.

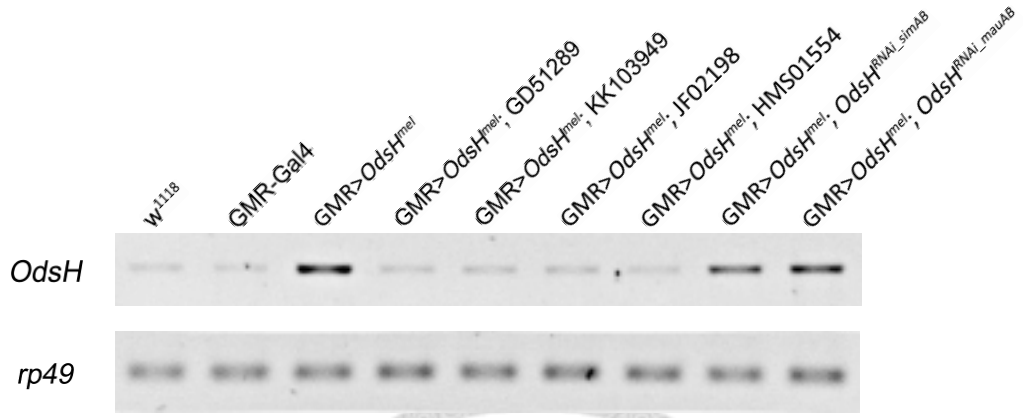

Figure 8. RT-PCR detection of *OdsH*^{mel} expression in wild-type and transgenic male flies. Genotypes are indicated above the graph. *rp49* was used as a loading control.

His-GFP expression in testes of *OdsH*$^{+}$ and *OdsH*^{0} flies

To determine which testicular cells can be observed in the *his*-GFP background, it is necessary to clarify the construction of this transgenic line. *his*-GFP, synonymous with *His2AvD*-GFP, encodes a variant H2A.F/Z class histone of *D. melanogaster* fused with the green fluorescence protein of *Aequorea victoria*. Its localization to chromosomes makes it a superb reporter gene to visualize nuclear activity during interphase, mitosis and meiosis (CLARKSON and SAINT 1999; WHITE-COOPER 2004). In post-meiotic spermatids, chromatin undergoes reorganization and condensation; histones are modified, removed and replaced by protamines (JAYARAMAIAH RAJA and RENKAWITZ-POHL 2005; RATHKE *et al.* 2007). Therefore, in *his*-GFP testes, where GFP signal appears indicates an aggregate of chromosome in germ cells, including GSCs, spermatogonia, spermatocytes and early spermatids. The only somatic cells that can be easily observed are the dividing somatic stem cells (SSCs) and the newly divided somatic cyst cells. Unlike GSCs that undergo four rounds of mitosis and two rounds of meiosis, SSCs merely divide once during spermatogenesis, which makes them relatively few in number.

I first examined the His-GFP expression in the testes of *OdsH*$^{+}$ and *OdsH*^{0} flies to uncover how *OdsH* affects the male germ cells in general. Immediately, I noted that His-GFP displayed various expression patterns in *OdsH*$^{+}$ and *OdsH*^{0} testes at day 0. The distribution of His-GFP in testes was in the apical region (Figure 9, A and E), somewhat extending (Figure 9, B and F), or further extending towards the basal end (Figure 9, C and G). On the contrary, at day 32, His-GFP distribution was quite similar in *OdsH*$^{+}$ and *OdsH*^{0} testes (Figure 9, D and H), from the apical tip towards the distal end. Quantification assay showed a significantly higher GFP signal in *OdsH*$^{+}$ testes than in

OdsH^{0} testes at day 0, but not at day 32 (Figure 10).

Sa-GFP expression in testes of *OdsH*$^{+}$ and *OdsH*^{0} flies

Since I observed a significant difference of GFP expression between *OdsH*$^{+}$; *his*-GFP and *OdsH*^{0}; *his*-GFP, I investigated the expression pattern of Sa-GFP, a primary spermatocyte marker (CHEN *et al.* 2005), in testes of different ages by immunostaining (Figure 11, A-F). Quantification assay showed at days 1, 15 and 55, no significant difference of GFP signal in *sa*-GFP, *OdsH*$^{+}$ and *sa*-GFP, *OdsH*^{0} testes (Figure 12).

BamP-GFP expression in testes of *OdsH*$^{+}$ and *OdsH*^{0} flies

Next, I characterized the BamP-GFP expression pattern in testes of different ages. Immunostaining shows that, in both *OdsH*$^{+}$; *bamP*-GFP and *OdsH*^{0}; *bamP*-GFP testes, *bam* promoter-driven GFP expression either resembled the endogenous *bam* expression, which starts from the 4-cell cyst stage until the entry into premeiotic G_2 phase and peaks in 8-cell cysts (Figure 13, A-C and G-I), or displayed somewhat misimpression pattern that spread extensively from the apical region to the distal end (Figure 13, D-F and J-L). No quantification was done due to inconsistency in expression pattern.

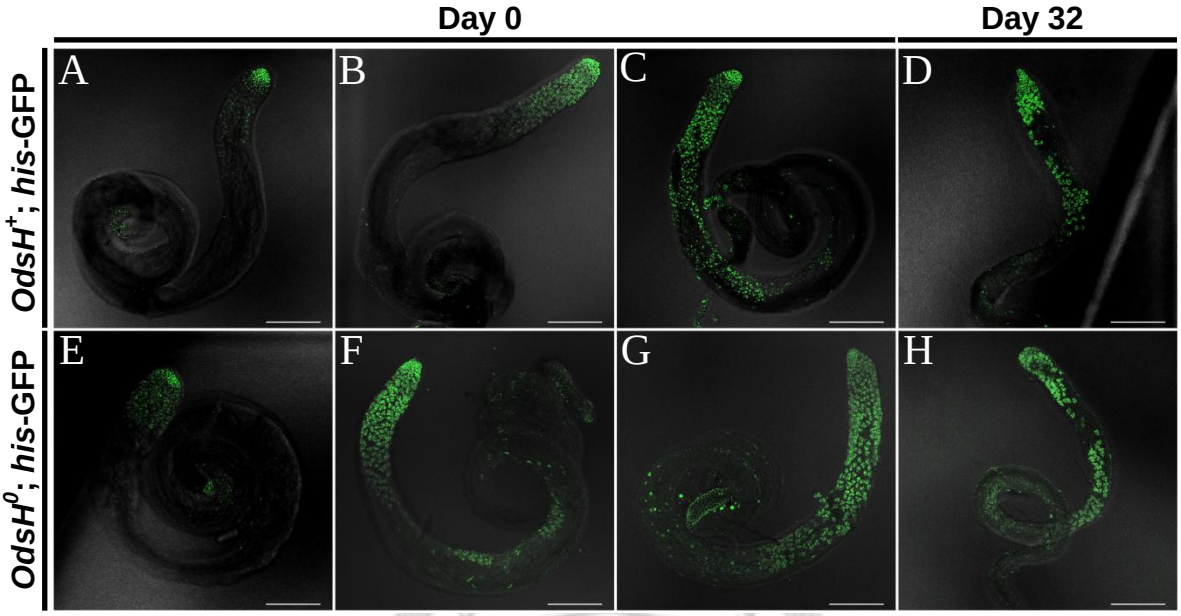

Figure 9. His-GFP expression in testes of 0- and 32-day-old *OdsH*$^{+}$ and *OdsH*^{0} flies. Testes from (A-C) 0- and (D) 32-day-old flies of *OdsH*$^{+}$; *his*-GFP and from (E-G) 0- and (H) 32-day-old flies of *OdsH*^{0}; *his*-GFP were shown. Testes were stained with anti-GFP (green). Scale bars: 100 μm.

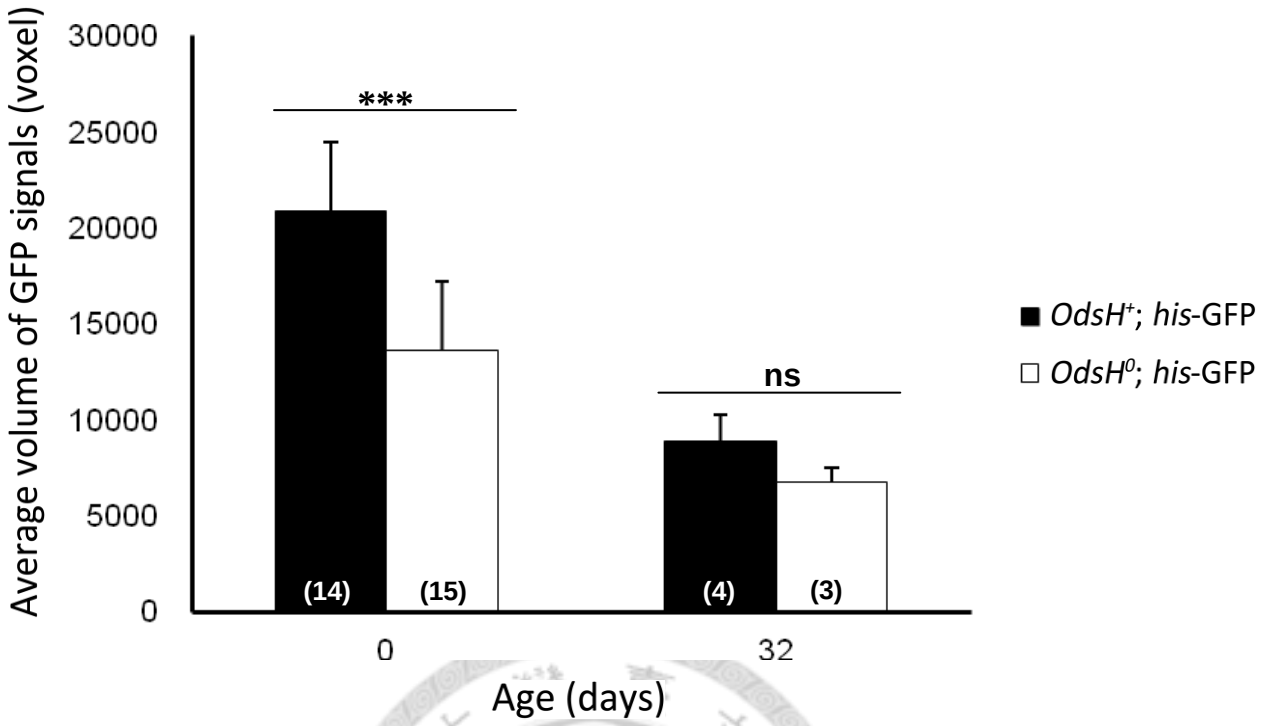

Figure 10. The average volume of His-GFP signal per testis. The histogram depicts the average volume of His-GFP signal per testis from *OdsH*$^{+}$; *his*-GFP and *OdsH*^{0}; *his*-GFP flies at 0 and 32 days of age. Numbers on the bars indicate the sample size for each genotype. Error bars indicate the standard deviation of the mean. Statistical significance was determined with the Mann-Whitney *U* test. ***, $P < 0.001$; ns, not significant.

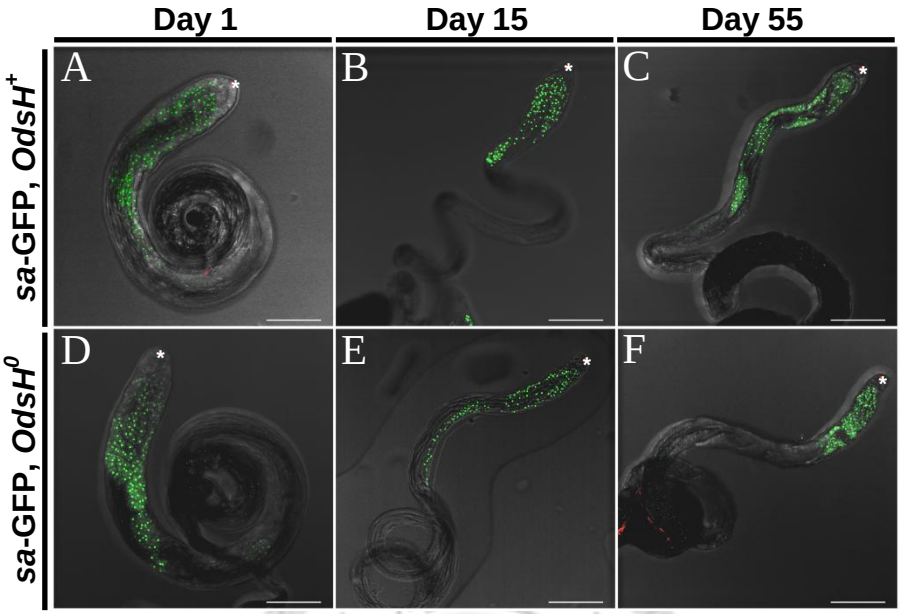

Figure 11. Sa-GFP expression in testes of 1-, 15-, and 55-day-old *OdsH*$^{+}$ and *OdsH*^{0} flies. Testes from (A) 1- (B) 15- and (C) 55-day-old flies of *sa*-GFP, *OdsH*$^{+}$ and from (D) 1- (E) 15- and (F) 55-day-old flies of *sa*-GFP, *OdsH*^{0} were shown. Testes were stained with anti-GFP (green) and anti-Fasciclin III (*, hub cells). Scale bars: 100 μm.

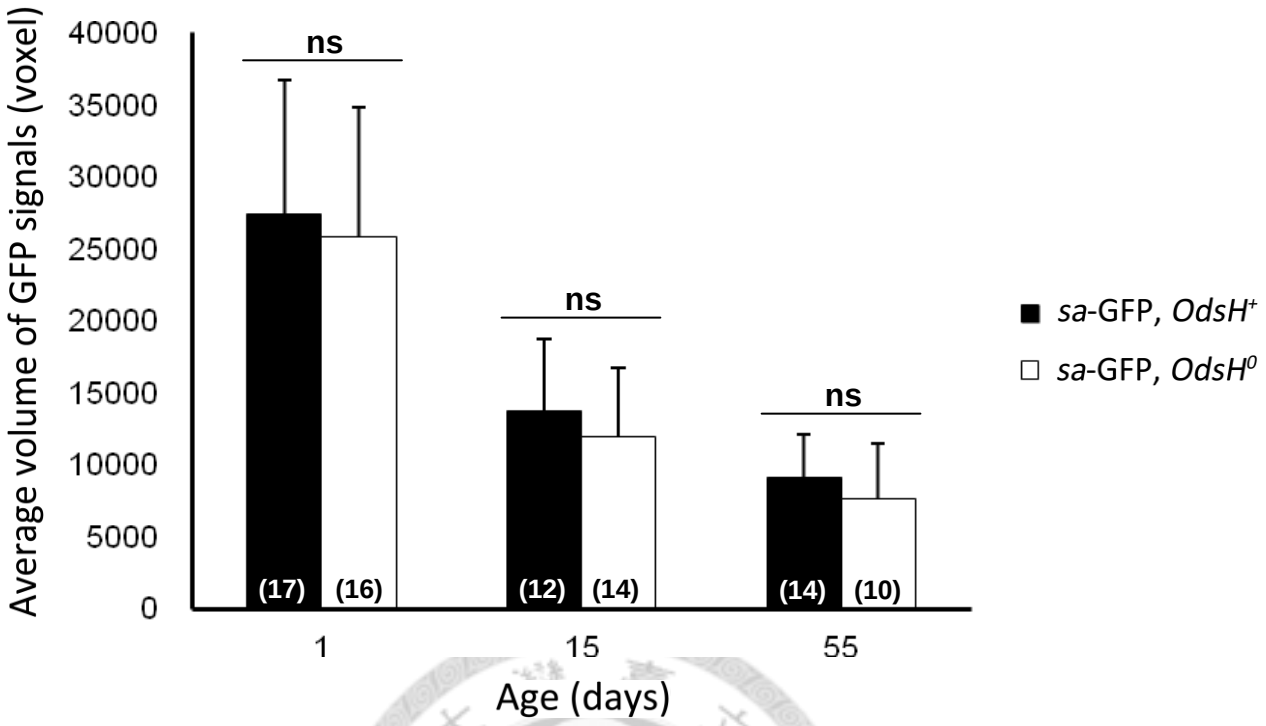

Figure 12. The average volume of Sa-GFP signals in spermatocytes. The histogram depicts the average volume of Sa-GFP signal in spermatocytes per testis from *sa*-GFP, *OdsH*$^{+}$ and *sa*-GFP, *OdsH*^{0} flies at 1, 15 and 55 days of age. Numbers on the bars indicate the sample size for each genotype. Error bars indicate the standard deviation of the mean. Statistical significance was determined with the Mann-Whitney *U* test. ns, not significant.

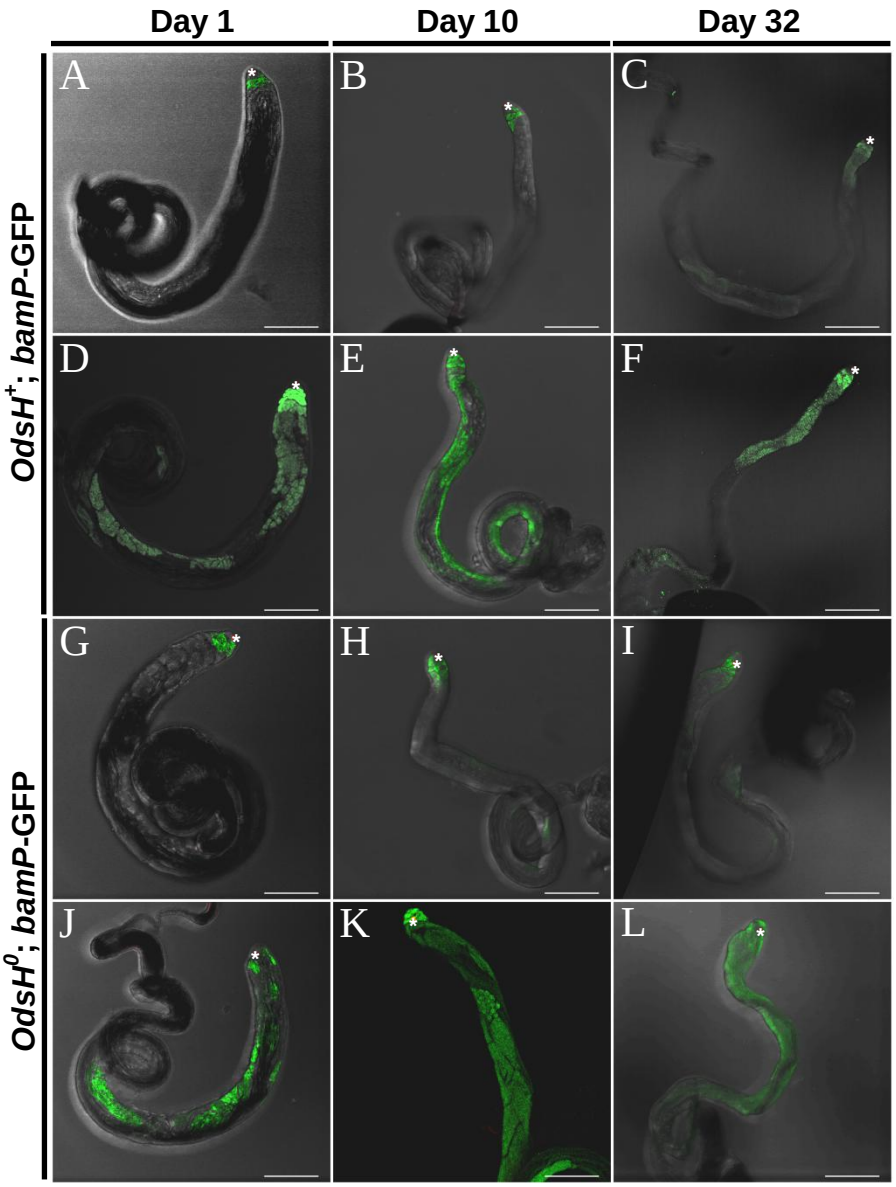

Figure 13. BamP-GFP expression in testes of 1-, 10-, and 32-day-old *OdsH*$^{+}$ and *OdsH*^{0} flies. Testes from (AD) 1- (BE) 10- and (CF) 32-day-old flies of *OdsH*$^{+}$; *bamP*-GFP and from (GJ) 1- (HK) 10- and (IL) 32-day-old flies of *OdsH*^{0}; *bamP*-GFP were shown. Testes were stained with anti-GFP (green) and anti-Fasciclin III (*, hub cells). Scale bars: 100 μm.

Discussion

OdsH RNAi strains should facilitate future studies on the functional divergence of duplicate genes and the normal function of *OdsH*^{sim}

Four *OdsH* RNAi strains from VDRC and TRiP were tested in *GMR>OdsH*^{mel} background. All of them rescued the ectopic expression phenotype to different levels, which indicates their efficiency. It seems unlikely to associate their efficiency with their targeting regions; all of the targeting regions fall within the exon 4 of *OdsH*, with one (JF02198 from TRiP) including the 3′ UTR (Figure 14 and Table 4). The observed less efficiency of GD51289 from VDRC is probably because the RNAi construct is generated via the *P*-element transformation, and its expression is subject to the position effect. Ultimately, these strains should be examined in a fertility assay to see whether their phenotype—males produce less offspring—shows consistency with *OdsH* null mutant. These strains should facilitate the simultaneous knockdown of *OdsH* and *unc-4* for future studies on the functional divergence between the two paralogs.

For the newly generated *OdsH*$^{RNAi\_simAB}$ and *OdsH*$^{RNAi\_mauAB}$, two target sites for each construct fall within the homeobox (mir-6-1-OdsH^{simA} and mir-6-1-OdsH^{mauA}) and the exon 4 (mir-6-1-OdsH^{simB} and mir-6-1-OdsH^{mauB}), respectively (Figure 14). Considering the sequence divergence of *OdsH* (Table 5), it is expected to see the incomplete rescue effect. Although the phenotypic rescue effect were observed, these two strains need to be further tested in the *GMR>OdsH*^{sim} and *GMR>OdsH*^{mau} background to determine the knockdown efficiency.

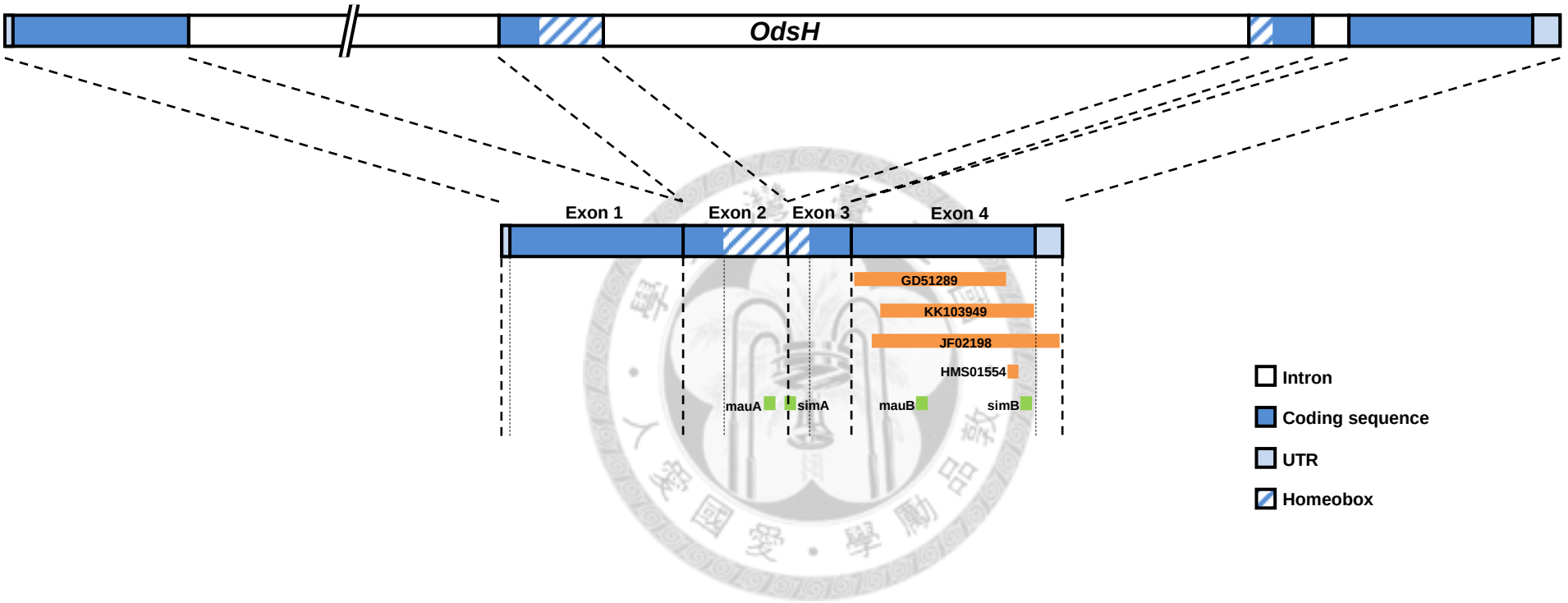

Figure 14. *OdsH* structure and the target regions of *UAS-OdsH*^{RNAi} strains used in this thesis. Self-made RNAi constructs (mir-6-1-OdsH^{simA}, mir-6-1-OdsH^{simB}, mir-6-1-OdsH^{mauA} and mir-6-1-OdsH^{mauB}) are denoted as simA, simB, mauA and mauB. Note that target regions of GD51289, HMS01554 and simB do not overlap.

Table 4. The target sequences of *UAS-OdsH^{RNAi}* strains obtained from stock centers. *OdsH* 3′ UTR is underlined.

Strain	Length (bp)	Sequence (5′ to 3′)
GD51289	328	CGCAGCAAGCGGATGAAGAAAGCCATCGATCGGCAGGCGAAGAAGCTACAGGACAAGGGATTGGAAGTGGACTATGCCCGTCTGGAGGCCGAGTACCTAG CTGCCCACCAGGAGAACGGAGTGGATGAGAATAACTGGCTGGATGATGATGGCTACGATGATCTGCACATCGATGTGGTGGGCGTTGAACCGGAGTACGT GACCGGCGACAGTTTGGATCACTCGTTCTGCTCCTCCAGGACGTACCAGACGAAGAGCACCAGCAGCGAACTGGATTCCAATGATATGGGACTCCAGGGA AGAGTGGAAACTCCGCCACCACCACAGC
KK103949	331	GACAAGGGATTGGAAGTGGACTATGCCCGTCTGGAGGCCGAGTACCTAGCTGCCCACCAGGAGAACGGAGTGGATGAGAATAACTGGCTGGATGATGATG GCTACGATGATCTGCACATCGATGTGGTGGGCGTTGAACCGGAGTACGTGACCGGCGACAGTTTGGATCACTCGTTCTGCTCCTCCAGGACGTACCAGAC GAAGAGCACCAGCAGCGAACTGGATTCCAATGATATGGGACTCCAGGGAAGAGTGGAAACTCCGCCACCACCACAGCCACCGATGCAGAATAAGACCCTC TACAATTCGCCCTTCAGCATCGAATCCCTGT
JF02198	405	AGCTACAGGACAAGGGATTGGAAGTGGACTATGCCCGTCTGGAGGCCGAGTACCTAGCTGCCCACCAGGAGAACGGAGTGGATGAGAATAACTGGCTGGA TGATGATGGCTACGATGATCTGCACATCGATGTGGTGGGCGTTGAACCGGAGTACGTGACCGGCGACAGTTTGGATCACTCGTTCTGCTCCTCCAGGACG TACCAGACGAAGAGCACCAGCAGCGAACTGGATTCCAATGATATGGGACTCCAGGGAAGAGTGGAAACTCCGCCACCACCACAGCCACCGATGCAGAATA AGACCCTCTACAATTCGCCCTTCAGCATCGAATCCCTGTTGGGATCGTAACGAATATCGAATGTTGTACTATAATTCTACTATGATTTCGGGTGGTTAGC TAAGC
HMS01554	21	CAGCAGCGAACTGGATTCCAA

Table 5. Homology of the target sequences of mir-6-1-based RNAi constructs in *Drosophila melanogaster*, *D. simulans* and *D. mauritiana*. The designed sequences are shown in bold letters. Mismatched nucleotides are indicated in red. Gaps are denoted as "-." Percentages in parentheses refer to the level of sequence homology in comparison with the designed sequence (number of identical matches divided by the sequence length).

	mir-6-1-OdsH^{mauA}	mir-6-1-OdsH^{simA}	mir-6-1-OdsH^{mauB}	mir-6-1-OdsH^{simB}
D. melanogaster	GGAGA**G**AG**T**CTTCCAGGGAA**G**T(86.4%)	ATAGCGGTTTGGT**TC**CA**G**AAT**C**(81.8%)	ATATGG**G**A**C**T**CC**A**G**G--GAA**G**A(63.6%)	AA**T**TCG**C**CCTTCAGCATC**G**AAT(86.4%)
D. simulans	GGAGA**G**AGCCTTCCAGGA**C**AAT(90.9%)	**ATAGCGGTTTGGTGTCAAAATA**	ATATGGAAGT**CC**A**G**G--GAATA(77.3%)	**AAATCGTCCTTCAGCATCAAAT**
D. mauritiana	**GGAGAAAGCCTTCCAGGAAAAT**	ATA**AA**G**A**T**A**TGGT**TC**CAAAATA(72.7%)	**ATATGGAAGTGGAAGTGGAATA**	AAATCGTCCTTCAGCATCAAAT (100%)

His-GFP expression implies GSC loss or disruption of subsequent spermatogenic development in young *OdsH^{0}* flies

Spermatogenesis in *D. melanogaster* is a series of cellular divisions and metamorphosis events. At the apex of a testis tub lies a group of somatic support cells termed hub cells, which are surrounded by 6-12 germline stem cells (GSCs) (SPRADLING *et al.* 2011). Each GSC is flanked by a pair of cyst progenitor cells (i.e. somatic stem cells, SSCs); both GSCs and SSCs are connected to the hub cells. As a GSC divides asymmetrically into two daughter cells, one maintains the GSC identity, and the other becomes a spermatogonium encapsulated by two somatic cyst cells. While these two cyst cells undergo no further division, the spermatogonium enters four rounds of synchronous mitotic division with incomplete cytokinesis, producing a cyst of 16 interconnected spermatogonia. The spermatogonia then embark on premeiotic DNA replication, and switch to an extended G_2 phase for cell growth as spermatocytes (LIM *et al.* 2012). During the G_2 phase, each spermatocyte substantially increases 25 times in volume. This premeiotic G_2 phase continues for more than 3 days before two meiotic divisions proceed, which generates 64 round spermatids (WHITE-COOPER 2010). Still interconnected by a cytoplasmic bridge (ring canal), these round spermatids subsequently enter the elongation program and become individual, mature sperms (Figure 15).

At day 0, His-GFP expression patterns were various in *OdsH^{+}* and *OdsH^{0}* testes. This is probably due to the individual variation. Because the development of testes starts in the late larval stage (CHENG *et al.* 2008), it is likely that flies collected on the same day differ in sexual maturation. The quantification difference of GFP signal indicates there are more cells (predominantly germ cells) in *OdsH^{+}* testes. One explanation

("explanation A") is that *OdsH*^{0} flies fail to maintain as many GSCs as *OdsH*$^{+}$ flies do, and GSC loss in *OdsH*^{0} testes causes a decrease in germ cell number. An alternative ("explanation B") is that the GSCs are intact, but the subsequent development in *OdsH*^{0} testes is disrupted. However, at day 32, the quantification of GFP shows no difference between *OdsH*$^{+}$ and *OdsH*^{0} testes. How does the age factor coordinate with these two explanations? One hypothesis is that the age effect on GSC maintenance, or the subsequent developmental stages, is accumulative and relatively minor than *OdsH*^{0} in young flies. In aged flies, *OdsH*^{0} effect is masked by the increasing age effect, so the germ cell number decreases in *OdsH*$^{+}$ and *OdsH*^{0} testes without significant difference. Both explanations are contradictory to the previous discovery that the GSC number is significantly less in 10-day-old, but not in 3-day-old, *OdsH*^{0} testes (CHENG *et al.* 2012).

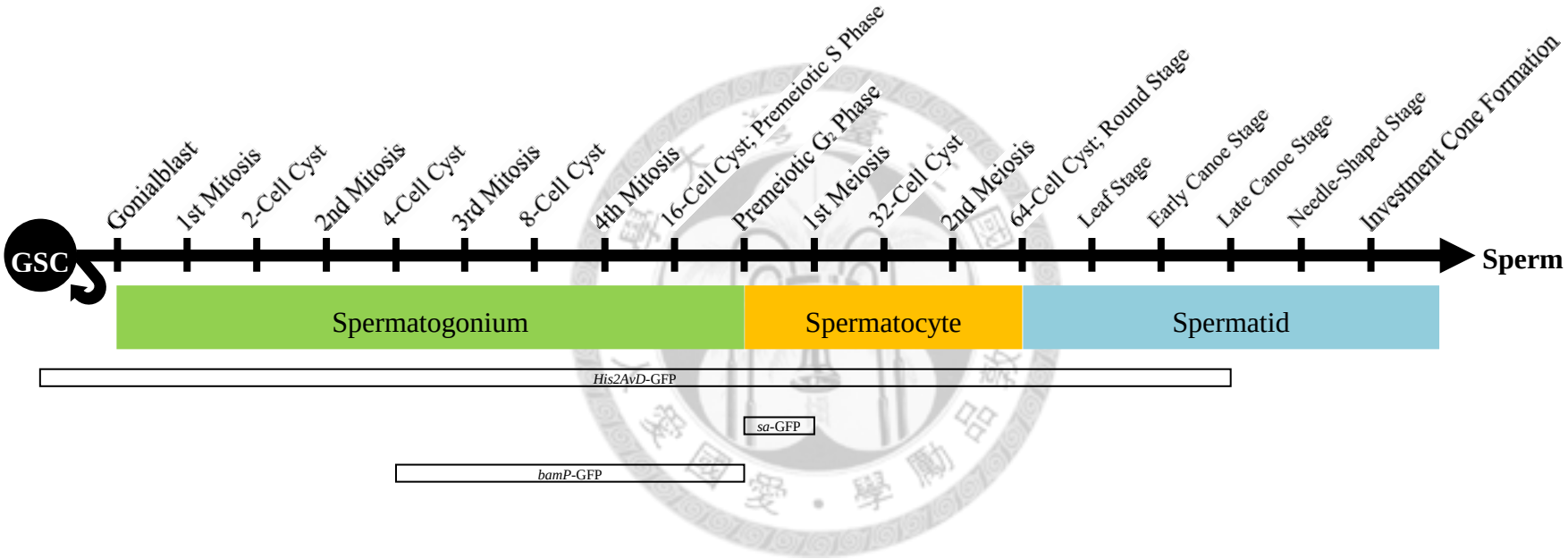

Figure 15. Male germline differentiation in *Drosophila melanogaster*. The schema is not in scale. Expression periods of three GFP reporter lines used in this study, *His2AvD*-GFP, *sa*-GFP and *bamP*-GFP, are indicated. Note that the various spermatid "stages" are defined by the nuclear shape, not mitochondrial.

Sa-GFP expression hints a possible role of *OdsH* in meiosis or spermatid differentiation

In early *Drosophila* spermatocytes, two classes of "meiotic arrest" genes have been identified and proved to be essential in meiotic divisions as well as spermatid differentiation (WHITE-COOPER *et al.* 1998). The meiotic arrest genes, named after the shared morphology of undifferentiated primary spermatocytes, are classified into *aly*- and *can*-class genes. The *aly*-class genes, including *always early* (*aly*), *achintya*/*vismay* (*achi*/*vis*), *cookie monster* (*comr*), *matotopetli* (*topi*) and *tombola* (*tomb*), constitute the testis-specific meiotic arrest complex (tMAC). tMAC is similar to *Drosophila* dREAM/MMB complex, an evolutionary conserved complex that exists in human and worm (WHITE-COOPER 2010). This complex functions as a transcriptional repressor and activator on a large number of developmentally regulated and cell-autonomous genes (GEORLETTE *et al.* 2007; LEWIS *et al.* 2004). tMAC consists of dREAM/MMB subunits (Caf1/p55 and Mip40), homologs of dREAM/MMB components (Aly [Mip130 homolog], Tomb [Mip120 homolog]), and the previous unknown (Comr and Topi) (LIM *et al.* 2012). The *can*-class genes encode testis-specific TAF (TBP-associated factor) homologs (tTAFs), including *cannonball* (*can*, TAF5 homolog), *meiosis I arrest* (*mia*, TAF6 homolog), *no hitter* (*nht*, TAF4 homolog), *ryan express* (*rye*, TAF12 homolog) and *sa* (TAF8 homolog) (LIM *et al.* 2012). In all eukaryotes, Transcription factor IID (TFIID) is the prototypical core promoter recognition factor. Comprised of the TATA-box-binding protein (TBP) and 13-14 TAFs, TFIID recognizes and binds core promoter elements such as the TATA box (through TBP), the initiator element (through TAF1 and TAF2), and the downstream promoter element (through TAF6 and TAF9), thus starting the formation of the RNA polymerase II transcription preinitiation complex.

It has been suggested that, in association with the prototypical core promoter recognition complexes, cell-type-specific TAFs play a crucial role in mediating cell-specific transcription and cell differentiation (GOODRICH and TJIAN 2010).

The roles of tMAC and tTAFs in *Drosophila* spermatogenesis have yet to be fully elucidated, but previous research works have showed an outline already. In general, tMAC regulates the entry into meiotic division, while tTAFs are associated with spermatid differentiation. Based on the observations on mutants, it is likely that tMAC acts upstream of tTAFs (WHITE-COOPER *et al.* 1998). tTAFs regulate the spermatid differentiation genes by 1) reducing the Polycomb group (PcG) binding to the target genes and 2) recruiting the Trithorax (TrxG) to the target genes (CHEN *et al.* 2005). PcG is related to gene silencing; one of its subunit, polycomb repressive complex 2 (PRC2) binds to the PcG target gene, creates trimethylation of histone H3 at lysine 27 (H3K27me3) marks and recruits PRC1 to repress gene expression by forming heterochromatin. TrxG catalyzes trimethylation of histone H3 at lysine 4 (H3K4me3) marks, which results in gene expression by forming euchromatin (JOBE *et al.* 2012). Also, in primary spermatocytes, tMAC is required for the localization of tTAFs to target genes and for the colocalization of tTAFs and PcG to a subcompartment within the nucleolus (CHEN *et al.* 2011).

sa is one of the *can*-class meiotic arrest genes. Quantification of Sa-GFP shows a declining trend of signal, but no significant difference between 1-, 15- and 55-day-old $OdsH^{+}$ and $OdsH^{0}$ testes. If the GFP intensity represents the cell number, there seems no difference in the total number of primary spermatocytes between $OdsH^{+}$ and $OdsH^{0}$ testes. This is, however, inconsistent with the two explanations for the *his*-GFP result, because in either case it is expected to see a significant difference between, at least,

1-day-old *OdsH*$^{+}$ and *OdsH*^{0} testes. Following explanation A (*OdsH*^{0} causes GSC loss in young flies), a wild guess is that knockout of *OdsH* upregulates *sa* expression in young *OdsH*^{0} flies, and this upregulation effect is compromised as *OdsH*^{0} flies age. Following explanation B (*OdsH*^{0} disrupts the subsequent spermatogenesis in young flies), it seems plausible when the disruption occurs after the primary spermatocyte stage (Figure 15), because the difference cannot be detected in *sa*-GFP background. Since *OdsH* expresses in the early stage of spermatogenesis (TING *et al.* 2004; VIBRANOVSKI *et al.* 2009), it is attractive to hypothesize that *OdsH* plays a role in the tMAC-tTAFs network. Knockout of *OdsH* causes a minor defect in meiosis and/or spermatid differentiation, and eventually leads to a decrease in germ cell number (Figure 16).

BamP-GFP expression yields no information on *OdsH* in early spermatogenesis

Either explanation A or B contradicts the previous study, which has demonstrated significant GSC loss in aged *OdsH*^{0} flies (CHENG *et al.* 2012). Therefore, it is necessary to examine the germ cells in early stage—GSCs and spermatogonia—in *OdsH*$^{+}$ and *OdsH*^{0} testes. *bamP*-GFP is a suitable reporter line to monitor the effect of *OdsH*^{0} on spermatogonia from the 4-cell to 16-cell cyst stage (GONCZY *et al.* 1997) (Figure 10). Unfortunately, at my hands, the pattern of BamP-GFP expression showed inconsistent. No matter how old the flies are, BamP-GFP in both *OdsH*$^{+}$ and *OdsH*^{0} testes either resembles the canonical pattern (a stripe of cells in the apical region of testes), or appears misexpressed throughout testes (Figure 13). This result hindered the further inference about the role of *OdsH* in early stages of spermatogenesis.

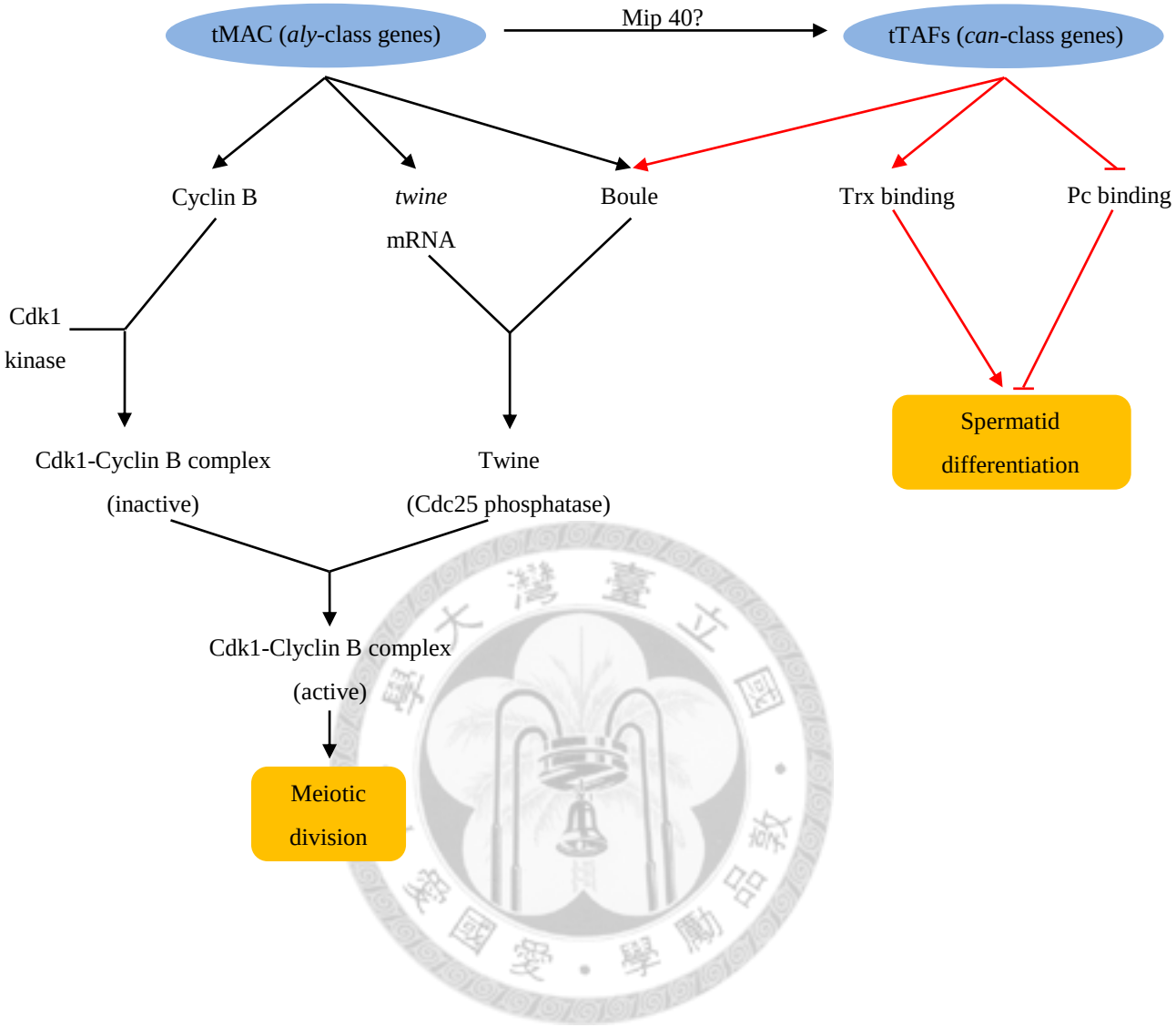

Figure 16. tMAC (*aly*-class genes) and tTAFs (*can*-class genes) network in *Drosophila melanogaster* spermatocytes.

References

AYALA, F. J., and W. M. FITCH, 1997 Genetics and the origin of species: an introduction. Proc Natl Acad Sci U S A **94:** 7691-7697.

BATESON, W., 1909 Heredity and variation in modern lights, pp. 85-101 in *Darwin and Modern Science*, edited by A. C. SEWARD. Cambridge University Press, Cambridge.

BAYES, J. J., and H. S. MALIK, 2009 Altered heterochromatin binding by a hybrid sterility protein in *Drosophila* sibling species. Science **326:** 1538-1541.

BROWNE, J., 2009 Darwin the scientist. Cold Spring Harb Symp Quant Biol **74:** 1-7.

CHARLESWORTH, B., and D. CHARLESWORTH, 2009 Darwin and genetics. Genetics **183:** 757-766.

CHEN, C.-H., H. HUANG, C. M. WARD, J. T. SU, L. V. SCHAEFFER *et al.*, 2007 A synthetic maternal-effect selfish genetic element drives population replacement in *Drosophila*. Science **316:** 597-600.

CHEN, D., and D. M. MCKEARIN, 2003 A discrete transcriptional silencer in the *bam* gene determines asymmetric division of the *Drosophila* germline stem cell. Development **130:** 1159-1170.

CHEN, X., M. HILLER, Y. SANCAK and M. T. FULLER, 2005 Tissue-specific TAFs counteract polycomb to turn on terminal differentiation. Science **310:** 869-872.

CHEN, X., C. LU, J. R. M. PRADO, S. H. EUN and M. T. FULLER, 2011 Sequential changes at differentiation gene promoters as they become active in a stem cell lineage. Development **138:** 2441-2450.

CHENG, J., N. TURKEL, N. HEMATI, M. T. FULLER, A. J. HUNT *et al.*, 2008 Centrosome misorientation reduces stem cell division during ageing. Nature **456:** 599-604.

CHENG, Y.-J., S. FANG, S.-C. TSAUR, Y.-L. CHEN, H.-W. FU *et al.*, 2012 Reduction of germ cells in the *Odysseus* null mutant causes male fertility defect in *Drosophila melanogaster*. Genes & Genetic Systems **87:** 273-276.

CLARKSON, M., and R. SAINT, 1999 A *His2AvDGFP* fusion gene complements a lethal *His2AvD* mutant allele and provides an *in vivo* marker for *Drosophila* chromosome behavior. DNA and Cell Biology **18:** 457-462.

COYNE, J. A., 1984 Genetic basis of male sterility in hybrids between two closely related species of *Drosophila*. Proc Natl Acad Sci U S A **81:** 4444-4447.

COYNE, J. A., and B. CHARLESWORTH, 1986 Location of an X-linked factor causing sterility in male hybrids of *Drosophila simulans* and *D. mauritiana*. Heredity (Edinb) **57 (Pt 2):** 243-246.

DANIELS, S. B., L. D. STRAUSBAUGH and R. A. ARMSTRONG, 1985 Molecular analysis of *P* element behavior in *Drosophila simulans* transformants. Molecular and general genetics **200:** 8.

DARWIN, C. R., 1859 *On the origin of species by means of natural selection, or the preservation of favoured races in the struggle for life*. John Murray, London.

DAVIS, R. H., 2004 The age of model organisms. Nature Reviews Genetics **5:** 69A-77.

DOBZHANSKY, T., 1936 Studies on hybrid sterility. II. Localization of sterility factors in *Drosophila pseudoobscura* hybrids. Genetics **21:** 113-135.

DOBZHANSKY, T., 1937 *Genetics and the Origin of Species*. Columbia University Press, New York.

GEORLETTE, D., S. AHN, D. M. MACALPINE, E. CHEUNG, P. W. LEWIS *et al.*, 2007

Genomic profiling and expression studies reveal both positive and negative activities for the *Drosophila* Myb-MuvB/dREAM complex in proliferating cells. Genes & Development **21:** 2880-2896.

GONCZY, P., E. MATUNIS and S. DINARDO, 1997 *bag-of-marbles* and *benign gonial cell neoplasm* act in the germline to restrict proliferation during *Drosophila* spermatogenesis. Development **124:** 4361-4371.

GOODRICH, J. A., and R. TJIAN, 2010 Unexpected roles for core promoter recognition factors in cell-type-specific transcription and gene regulation. Nature Reviews Genetics **11:** 549-558.

JAYARAMAIAH RAJA, S., and R. RENKAWITZ-POHL, 2005 Replacement by *Drosophila melanogaster* protamines and Mst77F of histones during chromatin condensation in late spermatids and role of sesame in the removal of these proteins from the male pronucleus. Mol Cell Biol **25:** 6165-6177.

JOBE, E. M., A. L. MCQUATE and X. ZHAO, 2012 Crosstalk among epigenetic pathways regulates neurogenesis. Frontiers in Neuroscience **6:** 1-15.

JOHNSON, N. A., 2008 Hybrid incompatibility and speciation. Nature Education **1(1)**.

KEYNES, M., and T. M. COX, 2008 William Bateson, the rediscoverer of Mendel. Journal of the Royal Society of Medicine **101:** 104-104.

LEWIS, P. W., E. L. BEALL, T. C. FLEISCHER, D. GEORLETTE, A. J. LINK *et al.*, 2004 Identification of a *Drosophila* Myb-E2F2/RBF transcriptional repressor complex. Genes & Development **18:** 2929-2940.

LIM, C., L. TARAYRAH and X. CHEN, 2012 Transcriptional regulation during *Drosophila* spermatogenesis. Spermatogenesis **2:** 158-166.

LIN, P.-C., 2009 Ectopic expression of *Odysseus* causes mitotic defects. Master's thesis. National Taiwan University, Taiwan.

LU, X., J. A. SHAPIRO, C.-T. TING, Y. LI, C. LI *et al.*, 2010 Genome-wide misexpression of X-linked versus autosomal genes associated with hybrid male sterility. Genome Research **20:** 1097-1102.

MAYR, E., 1942 *Systematics and the Origin of Species*. Columbia University Press, New York.

MCCARTHY, E. M., 2008 *On the Origins of New Forms of Life*. Eugene M. McCarthy, Macroevolution.net.

MULLER, H. J., 1942 Isolating mechanisms, evolution, and temperature. Biol. Symp.**:** 55.

NI, J.-Q., M. MARKSTEIN, R. BINARI, B. PFEIFFER, L.-P. LIU *et al.*, 2008 Vector and parameters for targeted transgenic RNA interference in *Drosophila melanogaster*. Nature Methods **5:** 49-51.

NI, J.-Q., R. ZHOU, B. CZECH, L.-P. LIU, L. HOLDERBAUM *et al.*, 2011 A genome-scale shRNA resource for transgenic RNAi in *Drosophila*. Nature Methods **8:** 405-407.

ORR, H. A., 1996 Dobzhansky, Bateson, and the genetics of speciation. Genetics **144:** 1331-1335.

PEREZ, D. E., and C.-I. WU, 1995 Further characterization of the *Odysseus* locus of hybrid sterility in *Drosophila*: one gene is not enough. Genetics **140:** 201-206.

PEREZ, D. E., C.-I. WU, N. A. JOHNSON and M.-L. WU, 1993 Genetics of reproductive isolation in the *Drosophila simulans* clade: DNA marker-assisted mapping and characterization of a hybrid-male sterility gene, *Odysseus* (*Ods*). Genetics **134:** 261-275.

RATHKE, C., W. M. BAARENDS, S. JAYARAMAIAH-RAJA, M. BARTKUHN, R. RENKAWITZ *et al.*, 2007 Transition from a nucleosome-based to a protamine-based chromatin configuration during spermiogenesis in *Drosophila*. Journal of Cell Science **120:** 1689-1700.

SINGH, S. R., and S. X. HOU, 2008 Immunohistological techniques for studying the *Drosophila* male germline stem cell. Methods Mol Biol **450:** 45-59.

SPRADLING, A., M. T. FULLER, R. E. BRAUN and S. YOSHIDA, 2011 Germline stem cells. Cold Spring Harbor Perspectives in Biology **3:** a002642.

SUN, S., C.-T. TING and C.-I. WU, 2004 The normal function of a speciation gene, *Odysseus*, and its hybrid sterility effect. Science **305:** 81-83.

TABUCHI, K., S. YOSHIKAWA, Y. YUASA, K. SAWAMOTO and H. OKANO, 1998 A novel *Drosophila* paired-like homeobox gene related to *Caenorhabditis elegans unc-4* is expressed in subsets of postmitotic neurons and epidermal cells. Neuroscience Letters **257:** 49-52.

THUMMEL, C. S., and V. PIRROTTA, 1992 Technical notes: new pCaSpeR *P*-element vectors. Drosophila Information Service **71:** 150.

TING, C.-T., S.-C. TSAUR, S. SUN, W. E. BROWNE, Y.-C. CHEN *et al.*, 2004 Gene duplication and speciation in *Drosophila*: evidence from the *Odysseus* locus. Proc Natl Acad Sci U S A **101:** 12232-12235.

TING, C.-T., S.-C. TSAUR, M.-L. WU and C.-I. WU, 1998 A rapidly evolving homeobox at the site of a hybrid sterility gene. Science **282:** 1501-1504.

VENKEN, K. J. T., Y. HE, R. A. HOSKINS and H. J. BELLEN, 2006 P[acman]: A BAC transgenic platform for targeted insertion of large DNA fragments in *D. melanogaster*. Science **314:** 1747-1751.

VIBRANOVSKI, M. D., H. F. LOPES, T. L. KARR and M. LONG, 2009 Stage-specific expression profiling of *Drosophila* spermatogenesis suggests that meiotic sex chromosome inactivation drives genomic relocation of testis-expressed genes. Plos Genetics **5:** e1000731.

WHITE-COOPER, H., 2004 Spermatogenesis: analysis of meiosis and morphogenesis. Methods Mol Biol **247:** 45-75.

WHITE-COOPER, H., 2010 Molecular mechanisms of gene regulation during *Drosophila* spermatogenesis. Reproduction **139:** 11-21.

WHITE-COOPER, H., M. A. SCHAFER, L. S. ALPHEY and M. T. FULLER, 1998 Transcriptional and post-transcriptional control mechanisms coordinate the onset of spermatid differentiation with meiosis I in *Drosophila*. Development **125:** 125-134.

Appendix I: RNAi constructs for transgenesis in *Drosophila simulans*

Generation of pCaSpeR4-based RNAi vectors for *P*-element transformation

On account of the uncertain effect of ΦC31 integrase on *D. simulans*, an alternative approach is the *P*-element transformation. To cut the RNAi constructs from pV22_OdsH^{simAB} and pV22_OdsH^{mauAB}, two criteria were used to choose the appropriate restriction enzymes: (1) to preserve the complete design in the original vector Valium22 and (2) to minimize the useless vector backbone in the excised fragment. Two restriction enzymes, *Stu*I and *Pvu*II, were thus selected to excise the RNAi constructs, and *Stu*I to linearize pCaSpeR4, the *P*-element transformation vector (THUMMEL and PIRROTTA 1992). Blunt-end ligation of the two fragments, though worked perfectly *in silico*, never *in vitro* (Figure 17).

Generation of *attB*-P[acman]-based RNAi vectors for *P*-element transformation by recombineering

The failure in pCaSpeR4 further catalyzed the idea to swap the RNAi constructs into the *attB*-P[acman] vector through recombineering-mediated gap repair (VENKEN *et al.* 2006). Two primer pairs, LA_F/LA_R and RA_F/RA_R, were designed according to the 5-prime and 3-prime end sequences of the gypsy-flanking region in pV22_OdsH^{simAB} and pV22_OdsH^{mauAB} (Figure 18, A). These two primer pairs were used to generate two ~500-bp fragments, named LA (left arm) and RA (right arm), with specific restriction enzyme sites, *Asc*I and *Pac*I, added to 5-prime end of LA and 3-prime end of RA. LA and RA were annealed together by PCR with the primers LA_F and RA_R (Figure17, B). The resulting ~1-kb PCR product was cloned into pCR™4-TOPO® TA vector (Invitrogen) and confirmed by sequencing. This 1-kb

fragment was then subcloned into *attB*-P[acman]-Cm^R (obtained from the *Drosophila* Genomics Resource Center at Indiana University), a chloramphenicol-resistant BAC vector that contains restriction recognition sites for *P*-transposase and ΦC31 integrase as well. The product was named gypsy_*attB*-P[acman]-Cm^R (Figure 18, C).

SW102 (a gift from Yikang Rong at the National Cancer Institute) is a tetracycline-resistant bacterial strain that encodes the heat-shock inducible λ-*Red* system for efficient homologous recombination. It was used to carry out recombineering-mediated gap repair. The donor plasmid pV22_$OdsH^{simAB}$ was first introduced into SW102 by electroporation, which was verified by the newly gained ampicillin resistance. This donor-containing SW102 was grown at 30°C overnight and incubated in a shaking waterbath at 42°C for 15 minutes before the subsequent electroporation of the *Bam*HI-linearized gypsy_*attB*-P[acman]-Cm^R. To identify successful recombination events, colony PCR was performed using primer pairs 5′-Check-F and 5′-Check-R, which are located at the backbone on *attB*-P[acman]-Cm^R and at the gypsy-flanking region on pV22_$OdsH^{simAB}$ respectively. However, no transformants were found (Figure 18, D-F).

My attempt at generating an RNAi line against $OdsH^{sim}$ has yet to succeed, because I failed to introduce the construct into pCaSpeR4 and *attB*-P[acman]-Cm^R, both of which are good for *P*-element transformation. Subcloning the mir-6-1-based RNAi design into pCaSpeR4 was always hampered by the blunt-end ligation; the key recombination in the recombineering-mediated gap repair method never occurred. However, concerning the obvious rescue effect demonstrated by $OdsH^{RNAi\_simAB}$ and $OdsH^{RNAi\_mauAB}$ in the *GMR>*$OdsH^{mel}$ background, it is reasonable to guess the RNAi construct will function in *Drosophila simulans*. It has been proved that *P*-element

transformation is feasible in *D. simulans* (DANIELS *et al.* 1985). Therefore, to bypass the problems with subcloning, I suggest the RNAi constructs be re-synthesized using newly designed primers with proper restriction recognition sites at both ends (Figure 1, B and C).

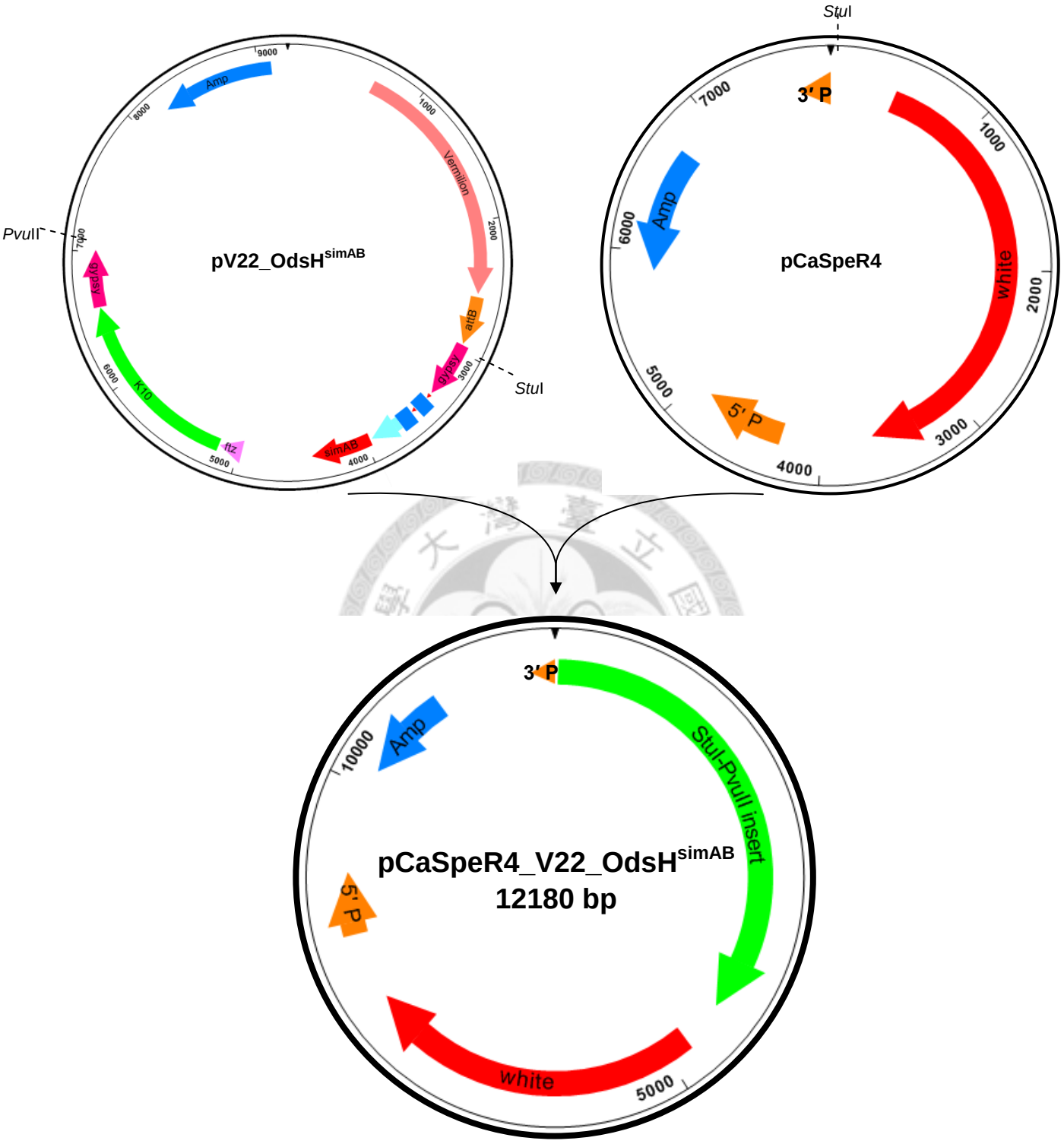

Figure 17. Design of pCaSpeR4_V22_OdsH^{simAB}, a pCaSpeR4-based RNAi vectors for *P*-element transformation. Both *Stu*I and *Pvu*II generate fragments with blunt ends.

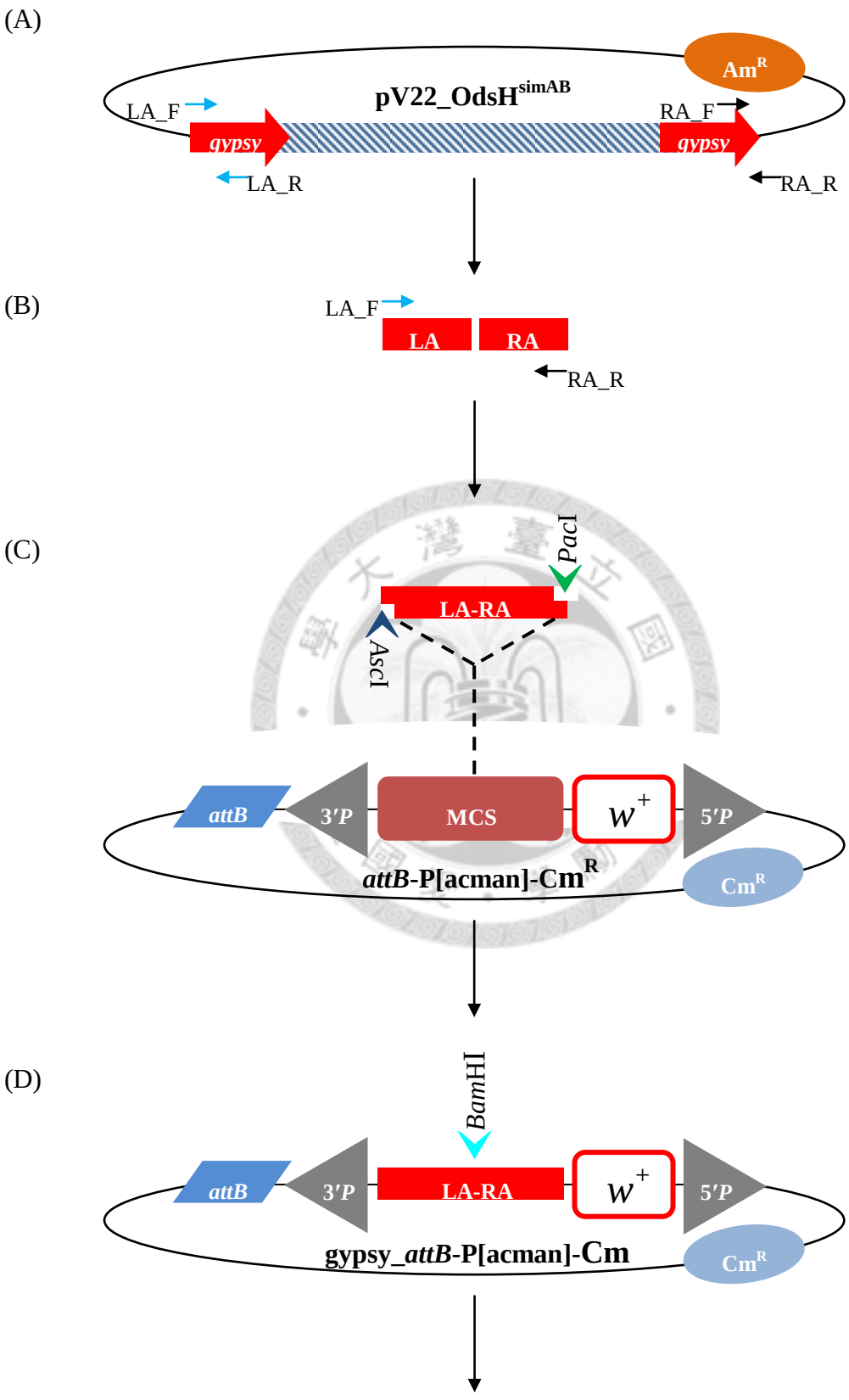

(continued on next page)

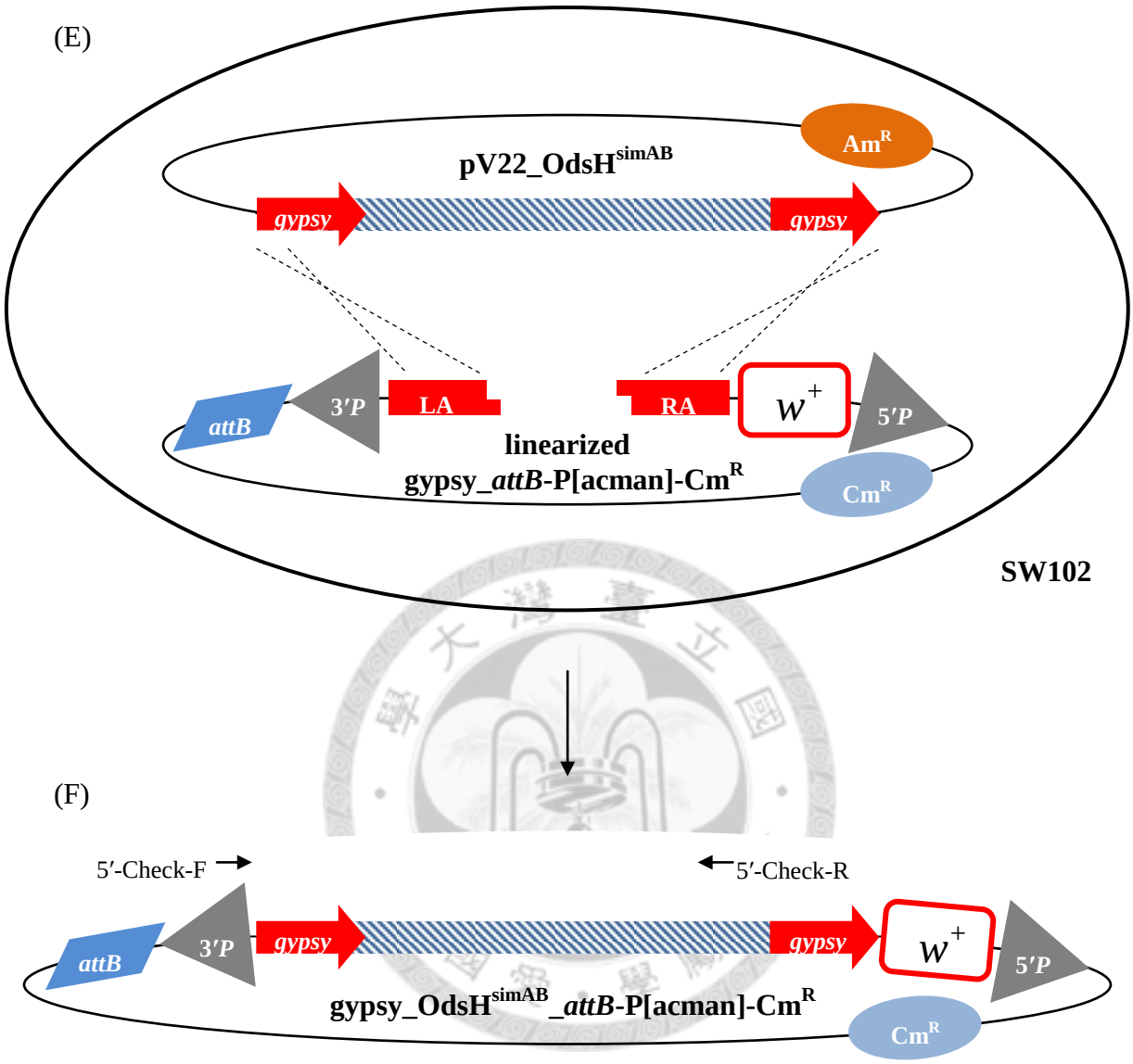

Figure 18. Retrival of miRNA construct against *OdsH*^{sim} from pV22_OdsH^{simAB} into *attB*-P[acman]-Cm^{R} by recombineering. (A) Two primer pairs were designed to amplify ~500-bp region of the 5-prime and 3-prime end of the gypsy-flanking fragment in pV22_OdsH^{simAB}. (B) The amplified fragments, LA and RA, were annealed by the second-round PCR. (C) The LA-RA fragment was cloned into *attB*-P[acman]-Cm^{R}, which generated gypsy_*attB*-P[acman]-Cm^{R}. (D) gypsy_*attB*-P[acman]-Cm^{R} was linearized at *Bam*HI site, and (E) transformed into the donor-containing SW102 bacterial strain by electroporation. (F) If the recombination occurs between the homology sequences at both ends, the gypsy-flanking fragment will be retrieved into *attB*-P[acman]-Cm^{R}. Successful recombination events can be examined by colony PCR using primer pairs 5′-Check-F and 5′-Check-R.

Appendix II: mir-6-1-based RNAi design

Pei Chun Lin, Chia-Hsiang Wu and Chau-Ti Ting

This new set of oligos are designed for generating a set of microRNAs which consist perfect match sequences to either *OdsH* or *unc-4* transcripts. The original idea comes from Dr. Chun-Hong Chen's work on *Meada* (CHEN *et al.* 2007). He also provided an instruction for the oligo design as attached at the end of this document. We plan to construct these engineered miRNAs into UASp for knockdown experiments. The goal is to generate miRNAs for $OdsH^{mel}$, $OdsH^{sim}$, $OdsH^{mau}$ and *unc-4*.

A target site on a target gene is selected according the criteria as follows: (1) a 22-nucleotide sequence, (2) a 30-52% guanine-cytosine content, (3) at least three adenine-thymine within the 16th to 20th nucleotide, (4) an adenine (**A**) at the 20th nucleotide, (5) no guanine at the 13th nucleotide, (6) an adenine at the 3rd nucleotide (optional), and (7) an thymine at the 10th nucleotide (optional). The resulting 22-nt sequence is then swapped to the Oligos 1 and 2 cassettes with the 20th nucleotide in the Oligo 1 replaced by cytosine (**C**). Then, the last four nucleobases of the Oligo 2 are changed to the reverse-complement counterpart of the last four nucleobases of the modified 22-nt sequence in Oligo 1. Anneal Oligos 1 and 2 by the first-round PCR, which generates the mir-6-1 mimic sequence that will later form the miRNA precursors in transgenic flies (Figure 1, A). This product is amplified by the second-round PCR with Oligos 3 and 4, which will add the mir-6-1 flanking sequences and restriction recognition sites *Not*I/*Bgl*II and *Bam*HI/*Xba*I at 5-prime and 3-prime ends respectively (Figure 1, B and C). The resulting PCR-amplified fragment needs to be confirmed by sequencing before cloned into any transformation vector. See Table 6 for oligo sequences and Table 7 for synthesized miRNA sequences.

Table 6. Oligo sequences for mir-6-1-based RNAi synthesis.

Name	Sequence (5′ to 3′)	Targeting region
Oligo 1		
miR6_unc4mel_A1	GGCAGCTTACTTAAACTTAATCACAGCCTTTAATGTCAATGCGTTCGCCAATCTA**C**CGTAAGTTAATATACCATATC	Exon 1 (CDS)
miR6_unc4mel_B1	GGCAGCTTACTTAAACTTAATCACAGCCTTTAATGTTCAAGGCCGAGTACATATC**C**CATAAGTTAATATACCATATC	Exon 4 (CDS)
miR6_unc4mel_C1	GGCAGCTTACTTAAACTTAATCACAGCCTTTAATGTCCAAAGCAATGCTTGAAAT**C**TGTAAGTTAATATACCATATC	Exon 4 (3′ UTR)
miR6_unc4mel_D1	GGCAGCTTACTTAAACTTAATCACAGCCTTTAATGTAGAGTCCATTTCTCATGGA**C**AGTAAGTTAATATACCATATC	Exon 4 (3′ UTR)
miR6_OdsHmel_A1	GGCAGCTTACTTAAACTTAATCACAGCCTTTAATGTTCATCCGCTTTGCAACTTT**C**CGTAAGTTAATATACCATATC	Exon 1 (CDS)
miR6_OdsHmel_B1	GGCAGCTTACTTAAACTTAATCACAGCCTTTAATGTCAGCCACCGATGCAGAATA**C**GATAAGTTAATATACCATATC	Exon 4 (CDS)
miR6_OdsHmel_C1	GGCAGCTTACTTAAACTTAATCACAGCCTTTAATGTGATTTCGGGTGGTTAGCTA**C**GCTAAGTTAATATACCATATC	Exon 4 (3′ UTR)
miR6_OdsHsim_A1	GGCAGCTTACTTAAACTTAATCACAGCCTTTAATGTATAGCGGTTTGGTGTCAAA**C**TATAAGTTAATATACCATATC	Exons 2 & 3 (CDS)
miR6_OdsHsim_B1	GGCAGCTTACTTAAACTTAATCACAGCCTTTAATGTAAATCGTCCTTCAGCATCA**C**ATTAAGTTAATATACCATATC	Exon 4 (CDS)
miR6_OdsHmau_A1	GGCAGCTTACTTAAACTTAATCACAGCCTTTAATGTGGAGAAAGCCTTCCAGGAA**C**ATTAAGTTAATATACCATATC	Exon 2 (CDS)
miR6_OdsHmau_B1	GGCAGCTTACTTAAACTTAATCACAGCCTTTAATGTTCGAGGATATGGAAGTGGA**C**GTTAAGTTAATATACCATATC	Exon 4 (CDS)
Oligo 2		
miR6_unc4mel_A2	AATAATGATGTTAGGCACTTTAGGTACCAATGCGTTCGCCAATCTA**A**CGTAGATATGGTATATTAACTTACGGT	Exon 1 (CDS)
miR6_unc4mel_B2	AATAATGATGTTAGGCACTTTAGGTACTCAAGGCCGAGTACATATC**A**CATAGATATGGTATATTAACTTATGGG	Exon 4 (CDS)
miR6_unc4mel_C2	AATAATGATGTTAGGCACTTTAGGTACCCAAAGCAATGCTTGAAAT**A**TGTAGATATGGTATATTAACTTACAGA	Exon 4 (3′ UTR)
miR6_unc4mel_D2	AATAATGATGTTAGGCACTTTAGGTACAGAGTCCATTTCTCATGGA**A**AGTAGATATGGTATATTAACTTACTGT	Exon 4 (3′ UTR)
miR6_OdsHmel_A2	AATAATGATGTTAGGCACTTTAGGTACTCATCCGCTTTGCAACTTT**A**CGTAGATATGGTATATTAACTTACGGA	Exon 1 (CDS)
miR6_OdsHmel_B2	AATAATGATGTTAGGCACTTTAGGTACCAGCCACCGATGCAGAATA**A**GATAGATATGGTATATTAACTTATCGT	Exon 4 (CDS)
miR6_OdsHmel_C2	AATAATGATGTTAGGCACTTTAGGTACGATTTCGGGTGGTTAGCTA**A**GCTAGATATGGTATATTAACTTAGCGT	Exon 4 (3′ UTR)
miR6_OdsHsim_A2	AATAATGATGTTAGGCACTTTAGGTACATAGCGGTTTGGTGTCAAA**A**TATAGATATGGTATATTAACTTATAGT	Exons 2 & 3 (CDS)
miR6_OdsHsim_B2	AATAATGATGTTAGGCACTTTAGGTACAAATCGTCCTTCAGCATCA**A**ATTAGATATGGTATATTAACTTAATGT	Exon 4 (CDS)
miR6_OdsHmau_A2	AATAATGATGTTAGGCACTTTAGGTACGGAGAAAGCCTTCCAGGAA**A**ATTAGATATGGTATATTAACTTAATGT	Exon 2 (CDS)
miR6_OdsHmau_B2	AATAATGATGTTAGGCACTTTAGGTACTCGAGGATATGGAAGTGGA**A**GTTAGATATGGTATATTAACTTAACGT	Exon 4 (CDS)
Oligo 3 and Oligo 4		
mi6_5′ NotI_BglII	GGCGCGGCCGCCGCCAGATCTTTTAAAGTCCACAACTCATCAAGGAAAATGAAAGTCAAAGTTGGCAGCTTACTTAAACTTA	
mi6_3′ BamHI_XbaI	GGCCTCTAGAACGGATCCAAAACGGCATGGTTATTCGTGTGCCAAAAAAAAAAAAAATTAAATAATGATGTTAGGCAC	

Table 7. Synthesized miRNA sequences.

Name	Sequence (5′ to 3′)
mir-6-1-unc4^{melA}	GGCGCGGCCGCCGCCAGATCTTTTAAAGTCCACAACTCATCAAGGAAAATGAAAGTCAAAGTTGGCAGCTTACTTAAACTTAATCACAGCCTTTAATGT**CAATGCGTT** **CGCCAATCTACCG**TAAGTTAATATACCATATCTA**CGTTAGATTGGCGAACGCATTG**GTACCTAAAGTGCCTAACATCATTATTTAATTTTTTTTTTTTTTGGCACACG AATAACCATGCCGTTTTGGATCCGTTCTAGAGGCC
mir-6-1-unc4^{melB}	GGCGCGGCCGCCGCCAGATCTTTTAAAGTCCACAACTCATCAAGGAAAATGAAAGTCAAAGTTGGCAGCTTACTTAAACTTAATCACAGCCTTTAATGT**TCAAGGCCG** **AGTACATATCCCA**TAAGTTAATATACCATATCTA**TGTGATATGTACTCGGCCTTGA**GTACCTAAAGTGCCTAACATCATTATTTAATTTTTTTTTTTTTTGGCACACG AATAACCATGCCGTTTTGGATCCGTTCTAGAGGCC
mir-6-1-unc4^{melC}	GGCGCGGCCGCCGCCAGATCTTTTAAAGTCCACAACTCATCAAGGAAAATGAAAGTCAAAGTTGGCAGCTTACTTAAACTTAATCACAGCCTTTAATGT**CCAAAGCAA** **TGCTTGAAATCTG**TAAGTTAATATACCATATCTA**CATATTTCAAGCATTGCTTTGG**GTACCTAAAGTGCCTAACATCATTATTTAATTTTTTTTTTTTTTGGCACACG AATAACCATGCCGTTTTGGATCCGTTCTAGAGGCC
mir-6-1-unc4^{melD}	GGCGCGGCCGCCGCCAGATCTTTTAAAGTCCACAACTCATCAAGGAAAATGAAAGTCAAAGTTGGCAGCTTACTTAAACTTAATCACAGCCTTTAATGT**AGAGTCCAT** **TTCTCATGGACAG**TAAGTTAATATACCATATCTA**CTTTCCATGAGAAATGGACTCT**GTACCTAAAGTGCCTAACATCATTATTTAATTTTTTTTTTTTTTGGCACACG AATAACCATGCCGTTTTGGATCCGTTCTAGAGGCC
mir-6-1-OdsH^{melA}	GGCGCGGCCGCCGCCAGATCTTTTAAAGTCCACAACTCATCAAGGAAAATGAAAGTCAAAGTTGGCAGCTTACTTAAACTTAATCACAGCCTTTAATGT**TCATCCGCT** **TTGCAACTTTCCG**TAAGTTAATATACCATATCTA**CGTAAAGTTGCAAAGCGGATGA**GTACCTAAAGTGCCTAACATCATTATTTAATTTTTTTTTTTTTTGGCACACG AATAACCATGCCGTTTTGGATCCGTTCTAGAGGCC
mir-6-1-OdsH^{melB}	GGCGCGGCCGCCGCCAGATCTTTTAAAGTCCACAACTCATCAAGGAAAATGAAAGTCAAAGTTGGCAGCTTACTTAAACTTAATCACAGCCTTTAATGT**CAGCCACCG** **ATGCAGAATACGA**TAAGTTAATATACCATATCTA**TCTTATTCTGCATCGGTGGCTG**GTACCTAAAGTGCCTAACATCATTATTTAATTTTTTTTTTTTTTGGCACACG AATAACCATGCCGTTTTGGATCCGTTCTAGAGGCC
mir-6-1-OdsH^{melC}	GGCGCGGCCGCCGCCAGATCTTTTAAAGTCCACAACTCATCAAGGAAAATGAAAGTCAAAGTTGGCAGCTTACTTAAACTTAATCACAGCCTTTAATGT**GATTTCGGG** **TGGTTAGCTACGC**TAAGTTAATATACCATATCTA**AGCTTAGCTAACCACCCGAAATC**GTACCTAAAGTGCCTAACATCATTATTTAATTTTTTTTTTTTTTGGCACACG AATAACCATGCCGTTTTGGATCCGTTCTAGAGGCC
mir-6-1-OdsH^{simA}	GGCGCGGCCGCCGCCAGATCTTTTAAAGTCCACAACTCATCAAGGAAAATGAAAGTCAAAGTTGGCAGCTTACTTAAACTTAATCACAGCCTTTAATGT**ATAGCGGTT** **TGGTGTCAAACTA**TAAGTTAATATACCATATCTA**TATTTTGACACCAAACCGCTAT**GTACCTAAAGTGCCTAACATCATTATTTAATTTTTTTTTTTTTTGGCACACG AATAACCATGCCGTTTTGGATCCGTTCTAGAGGCC
mir-6-1-OdsH^{simB}	GGCGCGGCCGCCGCCAGATCTTTTAAAGTCCACAACTCATCAAGGAAAATGAAAGTCAAAGTTGGCAGCTTACTTAAACTTAATCACAGCCTTTAATGT**AAATCGTCC** **TTCAGCATCACAT**TAAGTTAATATACCATATCTA**ATTTGATGCTGAAGGACGATTT**GTACCTAAAGTGCCTAACATCATTATTTAATTTTTTTTTTTTTTGGCACACG AATAACCATGCCGTTTTGGATCCGTTCTAGAGGCC
mir-6-1-OdsH^{mauA}	GGCGCGGCCGCCGCCAGATCTTTTAAAGTCCACAACTCATCAAGGAAAATGAAAGTCAAAGTTGGCAGCTTACTTAAACTTAATCACAGCCTTTAATGT**GGAGAAAGC** **CTTCCAGGAACAT**TAAGTTAATATACCATATCTA**ATTTTCCTGGAAGGCTTTCTCC**GTACCTAAAGTGCCTAACATCATTATTTAATTTTTTTTTTTTTTGGCACACG AATAACCATGCCGTTTTGGATCCGTTCTAGAGGCC
mir-6-1-OdsH^{mauB}	GGCGCGGCCGCCGCCAGATCTTTTAAAGTCCACAACTCATCAAGGAAAATGAAAGTCAAAGTTGGCAGCTTACTTAAACTTAATCACAGCCTTTAATGT**TCGAGGATA** **TGGAAGTGGACGT**TAAGTTAATATACCATATCTA**ACTTCCACTTCCATATCCTCGA**GTACCTAAAGTGCCTAACATCATTATTTAATTTTTTTTTTTTTTGGCACACG AATAACCATGCCGTTTTGGATCCGTTCTAGAGGCC